FACTORS AFFECTING THE DESIGN AND PERFORMANCE OF THE PM2.5 SAMPLER

A Dissertation

by

HUAN LI

Submitted to the Office of Graduate and Professional Studies of
Texas A&M University
in partial fulfillment of the requirements for the degree of

DOCTOR OF PHILOSOPHY

Chair of Committee,	Ronald E. Lacey
Committee Members,	Calvin B. Parnell
	John S. Haglund
	Maria D. King
Head of Department,	Steve Searcy

May 2017

Major Subject: Biological and Agricultural Engineering

ABSTRACT

Air pollution, especially particulate matter (PM), is of growing concern in the United States and around the world. PM with aerodynamic diameter (AED) less than 2.5μm is currently one of the two indicators for PM pollutions. The concentration of PM2.5 in ambient air is measured by the EPA-approved Federal Reference Method (FRM) or Federal Equivalent Method (FEM) PM2.5 sampler. The goal of this research was to study the factors affecting the design and performance of the PM2.5 sampler.

The key component of the PM2.5 sampler is the nozzle. Two sets of nozzles (40 nozzles per set) were tested in a sampler that was placed in a wind tunnel, and penetration efficiencies. It was shown that change in convergence angle of a modified nozzle can affect impactor performance. The √Stk50 for original and modified nozzles were 0.57 and 0.49, respectively. The slope of the efficiency curve for original and modified nozzles were 1.52 and 1.36, respectively.

During the wind tunnel test, the monodisperse aerosols were generated with artifacts known as multiplets and satellites. Two artifact correction methods, the Ranade method and the APS method, were compared experimentally and theoretically in this study. The two methods produced similar results in the wind tunnel tests, where the vibrating orifice aerosol generator was finely tuned to eliminate the satellites. However, in theoretical calculation, there were differences between these two methods. The APS method was able to completely correct for the effect of satellites since the APS provided data for the complete particle size distribution, which were used to identify satellites.

The Ranade method was found to be sensitive to satellites, especially for the larger particles where the sampling effectiveness was close to zero.

The lognormal distribution is widely used in the theoretical calculation and modeling of PM samplers; however, it was demonstrated that the error resulting from the lack of fit of the lognormal distribution was non-trivial. In this analysis, the error was as great as 22.68% when using a lognormal distribution. Ten distribution functions were applied to fit the performance curve given for FRM PM2.5 and PM10 samplers. The Kolmogorov Smirnov test and mass concentration calculation were used to demonstrate that the Dagum distribution provided the best fit among the ten functions.

DEDICATION

In memory of

Dr. Brock Faulkner

ACKNOWLEDGEMENTS

The past six years have been quite an adventure since I came to Aggie land. Along the way, a number of people made my research work possible and enjoyable.

Dr. Brock Faulkner, my primary research advisor, I always think of his smile when I visited him during his treatment at MD Anderson. His memory is an inspiration and source of strength for me in my life. I think of the simple conversations we had about experiments and life. His passion about air quality, his courage fighting with leukemia, they are memories I will cherish forever. He let me know the meaning of "It is not length of life, but depth of life".

After Dr. Faulkner passed away with a long battle with leukemia, a number of faculty members showed me guidance and support. Dr. Ron Lacey graciously served as my advisor and gave me full freedom to complete the work I had started under Dr. Faulkner's supervision. He inspired me to challenge the assumptions made in the research. Actually, the third objective in the dissertation was a result of casual talking with him. Dr. Calvin Parnell challenged my knowledge in air quality, especially in PM emission factor, and provided tremendous support. Dr. John Haglund and Dr. Maria King from mechanical engineering shared their expertise in aerosol science and provided moral support. Colonel Russell McGee also helped me to understand PM emission factors and shared stories about Dr. Faulkner.

Thanks are due to Allen Smith, Mathew Shimek, Walter Oosthuizen, Ahmad Kalbasi, and Gang Sun who collaborated with me on various projects. In addition, numerous past and present members of Parnell's crew at the Center for Agricultural Air

Quality Engineering and Science (CAAQES) have helped me to operate wind tunnel, aerosol generator, et al. Dr. John Wanjura at USDA helped me on the filter media project.

My landlord, Swiki Anderson shared his stories and encouraged me to continue to pursue the doctoral degree when I was at low tide. He told me half a PhD is not a PhD. Now I finally made it.

Last but not least, I would like to express gratitude to my parents, without their endless love and supports, this work would have never been even possible.

CONTRIBUTORS AND FUNDING SOURCES

Contributors

This work was supported by a dissertation committee consisting of Professor Ronald Lacey [advisor] and Calvin Parnell of Department of Biological and Agricultural Engineering and Research associate professor Maria King and Dr. John Haglund of the Department of Mechanical Engineering.

The nozzle design for Chapter II was provided by Dr. Haglund. The APS method for Chapter III was proposed by Dr. Haglund. The data used in Chapter V was provided by Dr. Parnell. The weight measurements of filter for appendix A was provided by Dr. John Wanjura at USDA.

All other work conducted for the dissertation was completed by the student independently.

Funding Sources

Graduate study was supported by the Texas Air Quality Initiative and the Cotton Foundation.

TABLE OF CONTENTS

Page

LIST OF FIGURES

Page

LIST OF TABLES

Page

CHAPTER I

INTRODUCTION

Particulate matter, also known as particle pollution or PM, is a complex mixture of extremely small solid particles and liquid droplets suspended in the air. PM2.5 is the fraction of particles suspended in the air with aerodynamic diameters that are nominally 2.5 μm and smaller. Aerodynamic diameter is the diameter of the spherical particle with a density of 1000 kg/m3 that has the same settling velocity as the particle (Hinds, 2012).

Epidemiological studies have consistently shown an association between particulate air pollution and not only exacerbations of illness in people with respiratory disease but also rises in the numbers of deaths from cardiovascular and respiratory disease among older people. (Seaton, 1995)

In order to protect the public from adverse effects of air pollution, the Clean Air Act was enacted by the United States Congress in 1970. Under the Clean Air Act, the Environmental Protection Agency (EPA) is required to set National Ambient Air Quality Standards (NAAQS) for pollutants considered harmful to public health and welfare. The mass concentration of PM2.5 are measured by EPA approved federal reference method (FRM) PM2.5 sampler.

OBJECTIVES

The goal of this research is to study the factors affecting the design and performance of the PM2.5 sampler. The objectives to address this goal are:

1. To study the effect of convergence angle on the impactor performance, (CHAPTER II)
2. To compare two multiplet correction methods, (CHAPTER III)
3. To quantify the error due to the lognormal distribution function fit the performance curve of PM2.5 sampler and propose other proper functions to provide better fit, (CHAPTER IV) and
4. To determine cumulative PM2.5 emission factor for agricultural operations using TSP concentration and particle size distribution data from Center for Agricultural Air Quality Engineering and Science. (CHAPTER V)

CHAPTER II

EFFECT OF CONVERGENCE ANGLE ON THE IMPACTOR PERFORMANCE

OVERVIEW

Two sets of nozzles were tested in a sampler that was placed in a wind tunnel, and penetration efficiencies, $\sqrt{Stk_{50}}$ and slope of the performance curve were determined by challenging the sampler with fluorescent-tagged monodisperse test aerosol particles having known concentration. It was shown that change in convergence angle of a modified nozzle can affect impactor performance. The $\sqrt{Stk_{50}}$ for original and modified nozzles were 0.57 and 0.49, respectively. The slope of the efficiency curve for original and modified nozzles were 1.52 and 1.36, respectively.

Keywords: inertial impactor, convergence angle, crossing trajectory phenomenon

INTRODUCTION

Inertial impactors are widely used to collect airborne particles for gravimetric or chemical analysis. Impactors have been studied extensively for different configurations and operational conditions. The key parameters of the inertial impactor are cutpoint and slope of the efficiency curve. In most ideal situations, the impactor would have a step-function efficiency curve, in which all particles larger than a certain size would be collected and all particles less than that size would pass through. However, in reality, oversize particles may pass through while undersize particles may become collected, resulting in an efficiency curve not “perfectly sharp” (Hinds, 2012).

Based on numerical methods solving the equations governing fluid flow and particle motion, for round impactors, the desired cutoff size is related to the number and size of nozzles and to the total volumetric flow rate (Marple and Willeke, 1976).

$$\boldsymbol{W = \sqrt{\frac{\rho_p \cdot Re}{9\rho \cdot Stk_{50}}} \cdot \sqrt{C} \cdot D_{50}} \quad (1)$$

Where, W is diameter of impactor, ρ_p is particle density, Re is Reynold's number, ρ is fluid density, Stk_{50} is the Stokes number value where sampling efficiency is 50%. C is slip correction factor, D_{50} is diameter at 50% collection efficiency.

John (1999) gave a simple derivation for the cutpoint of an impactor and showed that $\sqrt{Stk_{50}}$ values of 0.707 and 0.5 are appropriate for rectangular and circular nozzles, respectively. The collection efficiency of the impactor is governed by the dimensionless Stokes number, Stk,

$$\boldsymbol{Stk = \frac{\rho_p C V d_p^2}{9\mu D_j}} \quad (2)$$

Where, V is the air velocity at the nozzle exit, d_p is the diameter of particle, μ is fluid viscosity and D_j is nozzle diameter.

Jurcik and Wang (1995) found that the geometry of the impaction stage where the gas is accelerated does not affect the 50% cut size but has a strong effect on the sharpness and shape of the efficiency curve. This phenomenon is explained from the aerodynamic focusing effect of the particles in the nozzle (gas acceleration) section. The flat-plate orifice configuration, commonly used in cascade impactors, tends to focus particles closer to the centerline than the angled nozzle.

Hari et al. (2007) numerically studied the effect of the large particle crossing trajectory phenomenon on virtual impactor performance. The simulations reproduced trends of the experimentally observed performance including verification of a third region in the transmission efficiency curve, which is a drop-in transmission efficiency for large particle sizes. Visualization of simulated particle tracks show this decrease is attributed to a crossing trajectory phenomenon, whereby larger particles that acquire enough inertia in a chamfered acceleration nozzle, crossover the vertical mid-plane and impact on the opposite-side wall, particularly on the wall of the receiver section.

Most studies in the literature have focused mainly on the cut off size of the impactor, however, the steepness of the impactor performance curve can cause non-trivial changes in sampler performance as well. In the present study, the performance of an impactor was tested using two sets of nozzles with varying rates of convergence to investigate the effect of varying nozzle geometry on the steepness of the impactor performance curve.

METHODS

The performance of two nozzle designs varying in rate of convergence and throat length was tested in a high volume aerosol sampler. The sampler was challenged by solid ammonium fluorescein particles in a wind tunnel, and penetration efficiencies were determined by comparison of the collected aerosol mass on the filter from the sampler vs that of a reference sampler. The relative aerosol mass collected by each sampling device was established by fluorometric analysis.

Nozzle design

The two nozzles tested are shown in Figure 1. While the key parameter of the circular nozzle, the inner diameter, remained the same, there were other differences between the two nozzles:

- The rate of convergence of the airstream was decreased to reduce the lateral velocity of particles exiting the nozzle,
- The length of nozzle throat was shortened to reduce velocity loss due to friction along the nozzle wall, which also made the nozzle taper less aggressive to reduce the crossing trajectory phenomenon (Hari et al., 2007).
- Chamfering at the exit was eliminated,
- A ring was milled around the nozzle exit to reduce disturbance of particle trajectory by potential drag that may occur from the exit wall.

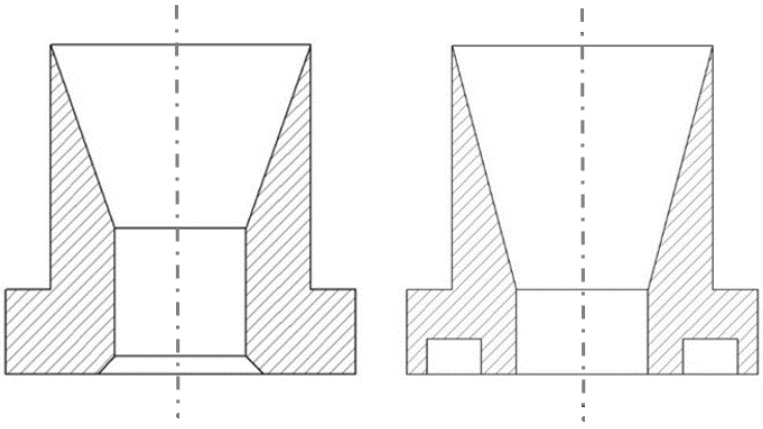

Figure 1 Nozzle profile (original nozzle on the left, modified nozzle on the right)

Wind tunnel

A wind tunnel was designed and fabricated at the Center for Agricultural Air Quality Engineering and Science (CAAQES) at Texas A&M University to achieve a uniform wind velocity and particle concentration (Table 1) as required to test samplers for Federal Reference Method (FRM) and Federal Equivalent Method (FEM) status according to 40 CFR Part 53 Subpart F. An overhead schematic of the wind tunnel is shown in Figure 2. The centrifugal fan (1) (PLR206, New York Blower Co., Willowbrook, IL) is equipped with a variable frequency drive to regulate the speed of the fan. The wind tunnel body is located on an elevated platform to minimize vibration effects. The fan blows air through a vertical transmission duct which leads to a horizontal duct (2). A vibrating orifice aerosol generator (3) is located inside a mixing chamber (4). A Sterman disc (5) is used to induce mixing of the air and aerosol particles, which then pass through a flow straightener (6) in the 1×1 m flow-stabilizing duct (7). At the end of this duct is the test chamber (8), which has an expanded cross sectional area to avoid wall effects and allow the base of the nozzles to be located outside of the test area. Air exiting the test chamber passes through a 90° exhaust elbow (9) which directs the flow out through an exhaust fan (10) on the roof of the building.

Table 1. Performance requirements for wind tunnels used for PM2.5 sampler performance testing

Parameter	Requirement
Wind speed	Mean wind speed is within ±10% for 2, 24 km/h
	Minimum of 12 test points
	Measuring techniques: precision ≤ 2% ; accuracy ≤ 5%
Particle concentration	The spatial variance (COV) is less than 10%
	Five or more evenly spaced isokinetic samplers
	Sampling zone: horizontal dimension > 1.2 times the width of the test sampler at its inlet opening
	Vertical dimension > 25 cm

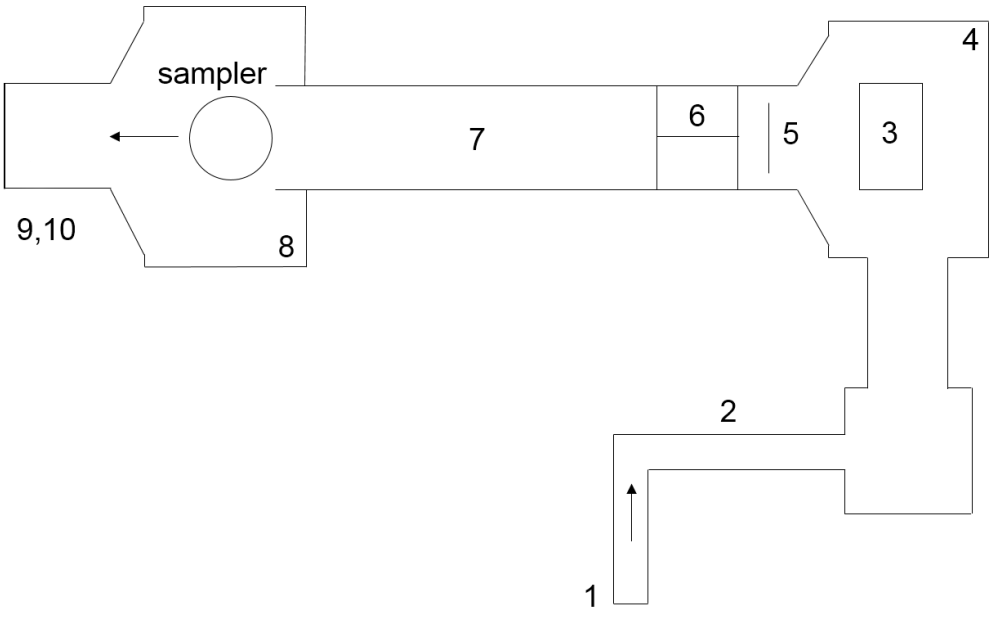

Figure 2. Schematic of the wind tunnel

Velocity uniformity

The velocity profile of the wind tunnel was measured using a hot wire anemometer (VelociCalc 8386, TSI, Inc., Shoreview, MN) with a precision of 0.01 m/s and an accuracy of ±1.5%. To obtain the velocity profile, the 1m×1m cross sectional area used for sampling was divided evenly into a 4×4 grid, and the velocity was measured at the center of each grid as shown in Figure 3. The anemometer was set to sample at a rate of 1Hz for 15 seconds and record the average wind speed across that time period. Twelve of these averages were taken at each point of the grid. Mean wind speeds in the test section were within ±10% of the target, and the variation at any test point in the test section did not exceed 10% of the measured mean (Table 2).

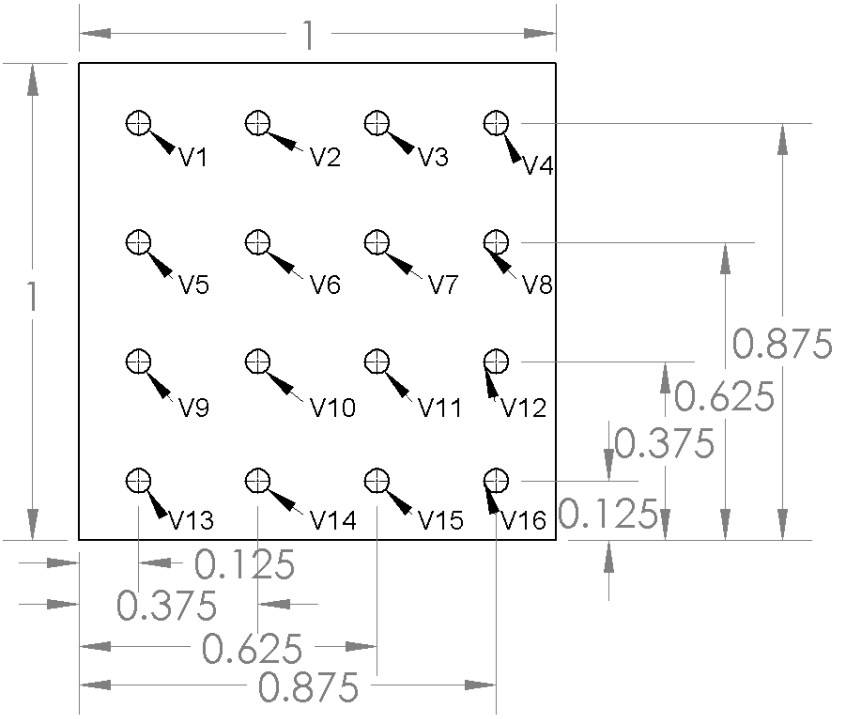

Figure 3. Test points of wind tunnel velocity uniformity tests (all units in meters)

Table 2. Velocity uniformity test results

Nominal Wind Speed (km/h)	Mean Wind Speed (km/h)	COV
2	1.92	1.8%
24	22.89	1.6%

Aerosol generation

A Vibrating Orifice Aerosol Generator (VOAG) was used to generate monodisperse, solid ammonium fluorescein particles. The components of VOAG system included a HPLC pump (Model 12-6, Scientific Systems Inc., State College, PA), frequency generator (4003A, BK Precision, Yorba Linda, CA), aerosol particle generator

(RNB Associates. Inc. Minneapolis, MN), and aerosol neutralizer (3054A, TSI Inc. Shoreview, MN).

Liquid solutions used to generate aerosols are composed of a known mass of fluorescein (CAS 2321-07-05) dissolved in ammonium hydroxide (NH4OH). When generated under proper conditions, the resulting particles are spherical and their aerodynamic diameter (AD) can be accurately calculated based on knowledge of the solution composition and the operational parameters of the VOAG (Berglund and Liu, 1973).

Verification of aerosol quality and size

Before each test, a glass slide (frosted slides 48312-003, VWR International, Radnor, PA) was prepared with a coating of silicon grease (high vacuum grease, Dow Corning, Midland, MI). This slide was then loaded into a glass slide impactor described by Faulkner and Haglund (2012). The glass slide impactor was placed into the test chamber and drew particle-laden air at a flow rate of 17 L/min through a 6.35 mm diameter orifice, which was 3.7 mm from the slide surface. The solid ammonium fluorescein particles that impacted the slide were collected by the silicon grease coating. The particles collected on glass slide were then measured under a microscope (Eclipse TS100, Nikon Instruments Inc., Melville, NY). At least 100 particles were sized for any given test. The populations of multiplets were analyzed by NIS-Elements Br Microscope Imaging Software (Nikon Instruments Inc., Melville, NY).

Between each test, particle-laden air was sampled with an Aerodynamic Particle Sizer (APS Model 3321, TSI, Inc., Shoreview, MN), which measured the aerodynamic

diameter distribution of the ammonium fluorescein particles, to make sure the particle distribution of each test was uniform and that the generation of satellite particles was minimized.

Concentration uniformity

A rack of nine isokinetic samplers was positioned in the test cross sectional area to measure the concentration uniformity of the wind tunnel. The 1m×1m cross sectional area used for sampling was divided evenly into a 3×3 grid, and the particle concentrations were measured at the center of each grid (Figure 4). The probes used for isokinetic samplers were machined conically from aluminum to hold 47 mm diameter filters. The inner surface of each nozzle was polished to reduce particle loss. The diameters of nozzles for 2 km/h and 24 km/h were 19.8 mm and 10.2 mm, respectively. The flow rates of each sampler were 10.3 L/min at 2 km/h wind speed and 32.4 L/min at 24 km/h wind speed.

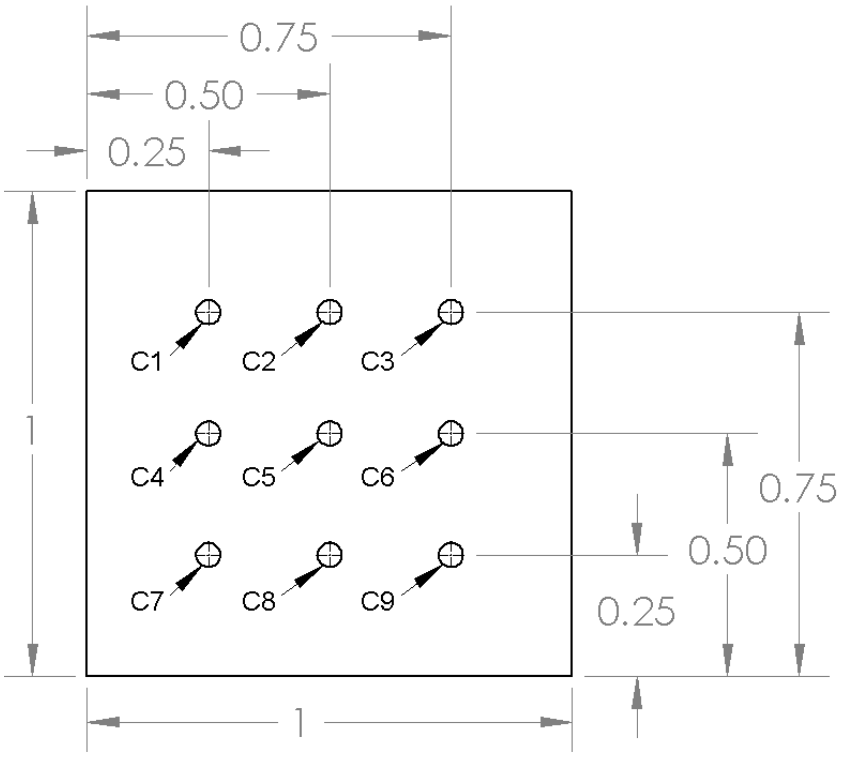

Figure 4. Test points for concentration uniformity tests (all measurements in meters)

For each wind speed, a VOAG was used to generate monodisperse solid ammonium fluorescein particles with aerodynamic diameters of 4μm in the wind tunnel. Particles were then collected for 1 hour at 2km/h wind speed and 2 hours at 24 km/h wind speed, using polytetrafluoroethylene (PTFE) filters ($PM_{2.5}$ Air Monitoring Membrane, Whatman, Maidstone, United Kingdom) placed in the isokinetic samplers. Three replicate data points were collected at each sampling location for each wind speed.

Each of these nine filters were then removed from the isokinetic samplers and placed into 125mL jars (Nalgene, Penfield, New York). To each jar was added 15 mL 0.01 mole/L ammonium hydroxide after the filter was placed into the jar. The jars were

soaked for a minimum of 4 hours before the solutions were analyzed with a fluorometer (Quantec model No. FM109515, Dubuque, Iowa). The fluorometer gave readings in Fluorescent Intensity Units (FIUs). An FIU is the uncalibrated output of the electrical signal conditioning circuit that processes the raw signal from the photomultiplier tube and is directly proportional to the concentration of the fluorescent tracer material.

Based on quality control parameters established by the authors (Faulkner et al., 2014), a fluorometric signal is considered reliable when the FIU value of the test solution is at least twice the FIU value of the 0.01 mole/L ammonium hydroxide solvent. Test durations varied from 1 to 2 hours to achieve a sufficient fluorometer reading. For 2 and 24 km/h wind speeds, the COV of the concentration was lower than 10% (Table 3), as required in 40 CFR 53 Subpart F for testing of FRM/FEM $PM_{2.5}$ samplers.

Table 3. Concentration uniformity test results

Nominal Wind Speed (km/h)	COV of Concentration
2	9.7%
24	9.1%

Test procedure

For any given test, particles were generated as described previously. Monodisperse aerosols with Stoke's numbers from 0.09 to 0.59 were then introduced into the wind tunnel, mixing with air. Following verification of aerosol size and quality, two isokinetic samplers containing 90 mm filters were placed in the wind tunnel at positions C2 and C5 as shown in Figure 4, and each sampler was connected to a pump

(Model G608NGX, General Electric commercial motors, Fairfield, CT). Following the connection of the pumps, the wind tunnel was turned on and the ambient wind speed was set. Isokinetic samplers were then turned on, and the flowrate adjusted to ensure isokinetic sampling conditions. The test sampler was then turned on, and the sampling time was set to 30 min for each test. Upon conclusion of each test, the isokinetic samplers were turned off. After each test, the filters were removed from the samplers, and were then placed into 0.01 mole/L ammonium hydroxide for fluorometric analysis. After a set of three consecutive tests were completed for a given particle size and wind speed, the VOAG system was flushed with pure ethanol to avoid clogging and contamination of subsequent tests.

The mass concentration of particles collected using each isokinetic sampler was calculated as:

$$\boldsymbol{C_{iso}} = \frac{\boldsymbol{FIU_{iso} \cdot m_{L,iso}}}{\boldsymbol{Q \cdot t}} \quad (3)$$

Where:

FIU_{iso} = average net fluorometric intensity of isokinetic sampler (FIU),

$m_{L,iso}$ = mass of liquid in which isokinetic filter was soaked (g),

Q = isokinetic sampler volumetric flow rate ($L \cdot min^{-1}$), and

t = sampling time (min).

The mass concentration of test sampler was calculated as:

$$C_{ts} = \frac{FIU_{ts} \cdot m_{L,ts}}{Q \cdot t} \quad (4)$$

Where:

FIU_{ts}= average net fluorometric intensity of test sampler (FIU),

$m_{L,ts}$ = mass of liquid in which test sampler filter was soaked (g),

Q = test sampler volumetric flow rate ($L \cdot min^{-1}$), and

t = sampling time (min).

The sampling effectiveness of test sampler was calculated as:

$$E = \frac{C_{ts}}{(C_{iso,1}+C_{iso,2})/2} \times 100\% \quad (5)$$

The coefficient of variation (CV_E) for the replicate sampling effectiveness measurements of the test sampler was calculated as:

$$CV_E = \frac{Standard\ Deviation\ of\ E}{average\ of\ E} = \frac{\sqrt{\frac{\sum_{i=1}^{3} E_i^2 - \frac{1}{3}\left(\sum_{i=1}^{3} E_i\right)^2}{2}}}{(E_1+E_2+E_3)/3} \times 100\% \quad (6)$$

Multiplet correction was based on techniques described by Marple et al. (1987).

RESULTS AND DISCUSSIONS

The multiplet-corrected effectiveness curves for two sets of nozzles are shown in Figure 5. The $\sqrt{Stk_{50}}$ for original and modified nozzles are 0.57 and 0.49, respectively. The $\sqrt{Stk_{50}}$ for the modified nozzle agrees well with the values obtained by Rader and Marple (1985), John (1999) and Hinds (2012). The ratio of diameters corresponding to 70% and 30% collection efficiency was used to describe the slope of the efficiency curve (Hillamo and Kauppinen, 1991). The diameters corresponding to 70% and 30% collection efficiency were determined by linear interpolation. The slope of the efficiency curve for original and modified nozzles were 1.52 and 1.36, respectively. Marjamäki et al. (2000) tested the performance of an electrical low pressure impactor and found that the slope of the efficiency curve varied from 1.09 to 1.31 with an average of 1.19. The

original impactor had a flatter performance curve than the modified nozzle due to the taper at exit which made the jet expand. As reported by Jurcik and Wang (1995), the geometry of the impaction stage significantly affected the slope of the performance curve. However, unlike the numerical results by Jurcik and Wang (1995), the geometry of the impaction stage also significantly affected the 50% cut size (or Stk_{50}). Larger particles that acquire enough inertia in a chamfered acceleration nozzle, crossover the vertical mid-plane and impact on the opposite-side wall (Hari et al. 2007). The velocity of these larger particles decreases after impaction, and these particles can pass through the impactor, leading to higher penetration efficiency as shown in Figure 5. For the modified nozzle, less aggressive nozzle taper reduces this crossing trajectory phenomenon.

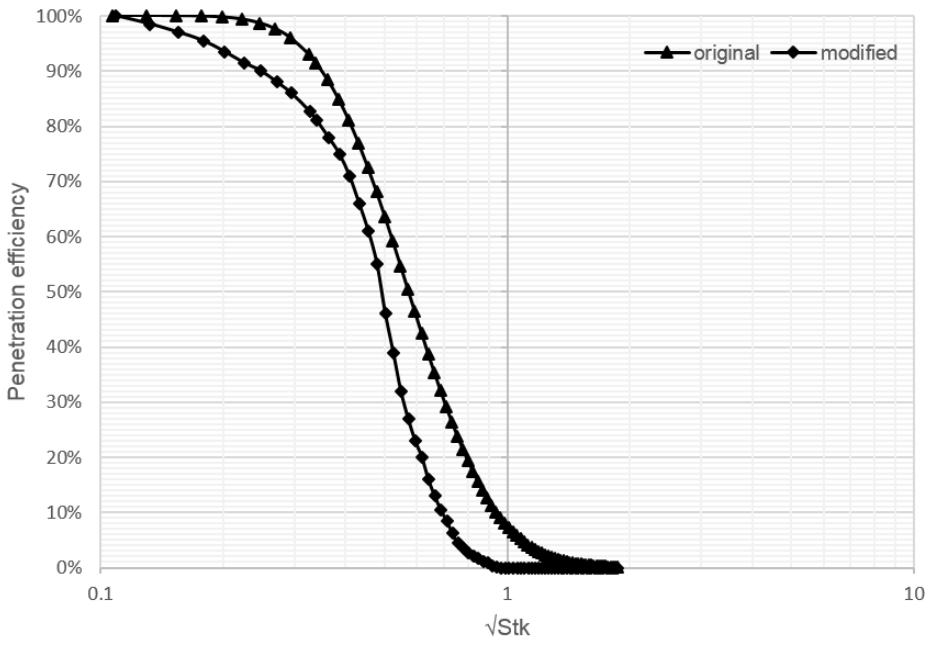

Figure 5. Penetration efficiencies of two sets of nozzles

Ratios of $\sqrt{Stk}_{10}$, $\sqrt{Stk}_{5}$, and $\sqrt{Stk}_{1}$ to $\sqrt{Stk}_{50}$, where $\sqrt{Stk}_{10}$, $\sqrt{Stk}_{5}$, and $\sqrt{Stk}_{1}$ are the square roots of Stokes number at penetration efficiencies of 10%, 5% and 1%, respectively, were calculated (Table 4). These ratios represent how far above the $\sqrt{Stk}_{50}$ value one must go before the nozzle achieves penetration efficiencies of 10%, 5% and 1%. All three ratios for the modified nozzle were smaller than the original nozzle, demonstrating that the modified nozzle performs better for eliminating larger particles as would be desirable in most industrial applications.

Table 4. Ratios of $\sqrt{Stk}_{10}$, $\sqrt{Stk}_{5}$, and $\sqrt{Stk}_{1}$ to $\sqrt{Stk}_{50}$.

Ratio	Original	Modified
$\sqrt{Stk}_{10}/\sqrt{Stk}_{50}$	1.65	1.41
$\sqrt{Stk}_{5}/\sqrt{Stk}_{50}$	1.91	1.52
$\sqrt{Stk}_{1}/\sqrt{Stk}_{50}$	2.49	1.77

CONCLUSIONS

Two sets of nozzles were tested in a sampler that was placed in a wind tunnel, and penetration efficiencies, $\sqrt{Stk}_{50}$ and slope of the performance curve were determined by fluorometric analysis. It was shown that even small changes in nozzle geometry that require the simplest changes in tooling can significantly affect impactor performance. While the key parameter, inner diameter, remained the same, small changes in convergence angle significantly affected Stk_{50} and slope of the performance curve. Less aggressive convergence angle can reduce the crossing trajectory phenomenon, thus improving the impactor performance for (i.e., reducing penetration of) particles larger than the cut point. After modification, the $\sqrt{Stk}_{50}$ of the nozzle decreased to 0.49, which

is the same for a well-designed impactor, regardless of the nozzle diameter or velocity (Hinds, 2012).

CHAPTER III

COMPARISON OF TWO CORRECTION METHODS FOR ARTIFACTS IN MONODISPERSE AEROSOLS

OVERVIEW

Monodisperse aerosols are widely used in calibration of particle sampling equipment but the process of generating these aerosols can produce artifacts of conjoined particles (multiplets) and fractional particles (satellites). These artifacts must be corrected for prior to using the data in an analysis of the sampling equipment. Two correction methods, the Ranade method and the aerodynamic particle sizer (APS) method were compared experimentally and theoretically in this study. The two methods yielded similar results in wind tunnel tests, where the vibrating orifice aerosol generator was finely tuned to eliminate the satellites. However, theoretical analysis of aerosols containing both satellites and multiplets exhibited differences between these two methods. The APS method corrected the effect of satellites since the APS provides all particle size distribution information. The Ranade method was sensitive to the presence of satellites, especially for larger particles, where the sampling effectiveness was close to zero.

Keyword: multiplets correction, VOAG, aerosol, wind tunnel, PM2.5

INTRODUCTION

Monodispersed aerosols are widely used in fundamental aerosol research, calibration of aerosol sampling, and measuring instruments. They are also used for

testing particulate control devices such as cyclones, filters, and scrubbers to determine the efficacy in reducing particulate air pollutant (Berglund and Liu, 1973). Monodisperse aerosols can be generated effectively by a vibrating orifice aerosol generator (VOAG); however, when using a VOAG some doublets (particles with twice the volume of singlets), triplets, and higher-order combinations are generated. Figure 6(a) shows APC data for particle size at the beginning of a test where the singlets are represented by the large peak at 4μm AED and a smaller quantity of doublets at 5μm AED. Figure 6(b) for data taken thirty minutes after the start of the test shows a change in particle size distribution (PSD), where a quantity of particles smaller than the desired diameter (i.e. satellites) were present.

Although the number of multiplets and satellites may be small relative to the total number of aerosol particles generated, their presence must be taken into consideration because of their different impaction characteristics. Marple et al. (1987) found that the collection efficiency of 2.1μm diameter particles was 11.3% with 4.5 and 0.5 percent doublets and triplets, respectively; while the actual efficiency was 1.8%. Therefore, in any Federal Reference Method (FRM) or Federal Equivalent Method (FEM) sampler performance test, it is required that the concentration of multiplets in the test aerosol must not exceed 10% (40 CFR Part 53). For a Class II FEM PM2.5 sampler, a correction for the presence of multiplets must be performed by the method of Marple et al. (1987) based on doublets and triplets. Ranade et al. (1990) provied more detailes how to perform this correction method.

Although the number of such multiplets may be small relative to the total number of aerosol particles generated, their presence must be taken into consideration due to their different impaction characteristics. Marple et al. (1987) found that the collection efficiency of 2.1 μm diameter particles was 11.3% with 4.5 and 0.5 percent doublets and triplets, respectively; while the actual efficiency was 1.8%. Therefore, in any Federal Reference Method (FRM) or Federal Equivalent Method (FEM) sampler performance test, it is required for the test aerosol that the population of multiplets must not exceed 10% (40 CFR Part 53). For a Class II FEM PM2.5 sampler, a correction for the presence of multiplets must be performed by the method of Marple et al. (1987) based on doublets and triplets.

The aerodynamic particle sizer (APS) became a commercial instrument in 1982 (Baron, 1986) and was the first commercial instrument to provide rapid, high resolution, real-time aerodynamic measurement of particles from 0.5 to 20 μm. The APS provides another way to perform the multiplet correction (Haglund et al., 2002). The main ideal of this method is based on the mass fraction of particles from 0.5 to 20 μm measured by the APS, detailed description will be discussed in the methodology section.

The goal of this study was to compare the proposed APS multiplet correction procedure with the method of Ranade et al. (1990) under different particle size distribution theoratcally and experimentally.

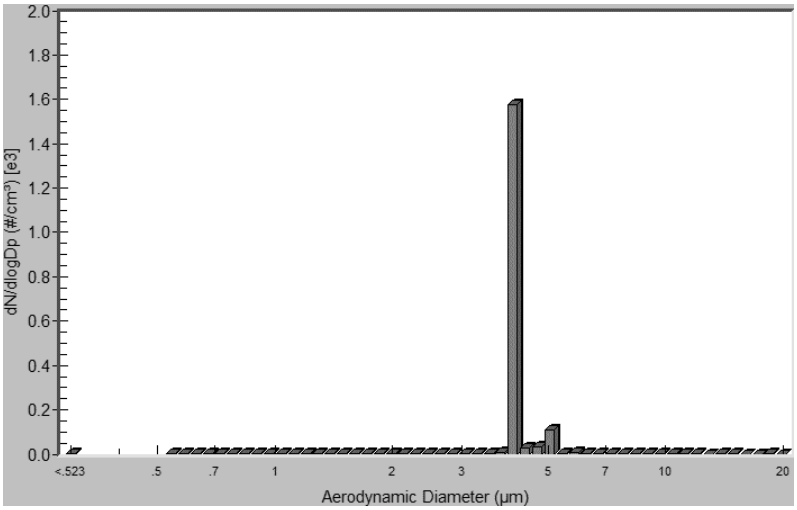

(a)

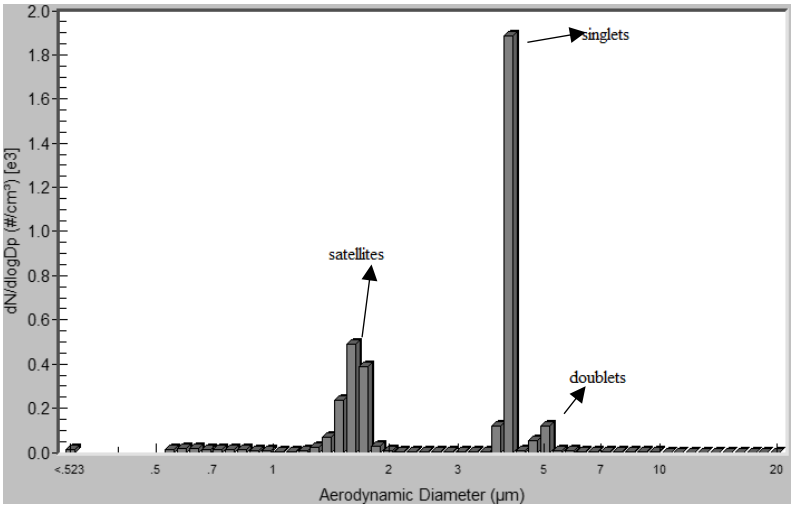

(b)

Figure 6. PSD of VOAG measured by APS, (a) at the beginning of test, (b) after half an hour later

METHODOLOGY

The collection effectiveness of a sampler is defined as:

$$\boldsymbol{E} = \frac{\boldsymbol{mass\ collected\ by\ sampler}}{\boldsymbol{mass\ collected\ by\ isokinetic\ sampler}} \times \mathbf{100}\% \qquad (7)$$

Due to the presence of doublets and triplets, the measured effectiveness can be described by

$$\mathbf{E_{act} = m_s E_s + m_d E_d + m_t E_t} \quad (8)$$

Where,

m_s, m_d and m_t are the mass fraction of singlets, doublets, and triplets, respectively; and E_s, E_d and E_t are the effectiveness of singlets, doublets, and triplets, respectively (Ranade et al., 1990).

Test setup

A wind tunnel was designed and fabricated at the Center for Agricultural Air Quality Engineering and Science (CAAQES) at Texas A&M University to achieve a uniform wind velocity and particle concentration as required to test samplers for FRM and FEM status according to 40 CFR Part 53 Subpart F. An overhead schematic of the wind tunnel is shown in Figure 2. The centrifugal fan (1) (PLR206, New York Blower Co., Willowbrook, IL) is equipped with a variable frequency drive to regulate the speed of the fan. The wind tunnel body is located on an elevated platform to minimize vibration effects. The fan blows air through a vertical transmission duct which leads to a horizontal duct (2). A vibrating orifice aerosol generator (3) is located inside a mixing chamber (4). A Sterman disc (5) is used to induce mixing of the air and aerosol particles, which then pass through a flow straightener (6) in the 1×1 m flow-stabilizing duct (7). At the end of this duct is the test chamber (8), which has an expanded cross sectional area to avoid wall effects and allow the base of the nozzles to be located outside of the test area. Air exiting the test chamber passes through a 90° exhaust elbow (9) which

directs the flow out through an exhaust fan (10) on the roof of the building. APS was placed next to the mixing chamber and measured the aerosol generated by VOAG.

Detailed test setup is available in the thesis of Li (2013).

Multiplets correction based on doublets and triplets (Ranade method)

The Ranade method is an iterative process based on the sampler effectiveness curve (i.e. the particle penetration values versus the aerodynamic particle diameter). The sampling effectiveness curve is drawn based on the uncorrected test data and the effectiveness values at each particle size for singlets, doublets, and triplets are determined from the uncorrected sampling effectiveness curve. Equation 2 is solved algebraically as a first approximation of the actual effectiveness for that experimental particle size. A second performance curve is drawn using the first approximation values for all particle sizes from the data set. This process is repeated at each particle size until the difference between successive approximations of the effectiveness values at each particle size are less than a predetermined value (Ranade et al., 1990). Note that there is no mechanism in this method to correct for satellites in the test aerosol.

Multiplets correction based on APS

A preliminary sampling effectiveness curve was determined by fitting a distribution function to the observed aerosol sampling effectiveness data by minimizing the sum of squared error (SSE) between predicted effectiveness and the data without multiplet correction. Sampling effectiveness values of 100% and 0% for particle size of 1 μm and 10 μm, respectively, were added to the observed data per the requirement of 40 CFR Part 53 Subpart F.

The sum of squared error (SSE) was calculated as:

$$\boldsymbol{SSE = \Sigma(E_i - \eta_{ex,i})^2} \quad (9)$$

Where

E_i=measured sampling effectiveness for particle size i, and

$\eta_{ex,i}$=expected (i.e., modeled) sampling effectiveness for particle size i.

Multiplet correction was then applied to sampling effectiveness data based on method described by Haglund et al. (2002). For each nominal particle size, measurements of particle size collected with the APS was used to quantify the relative mass concentrations of satellites and multiplets. A "particle size correction factor" (f) was calculated to correct APS-measured particle size data:

$$\boldsymbol{f = \frac{D_a}{D_{APS,VMD}}} \quad (10)$$

Where

D_a = calculated aerodynamic diameter of "monodisperse" particles based on VOAG parameter (μm), and

$D_{APS,\ VMD}$ = volume mean diameter reported by the APS (μm).

This particle size correction factor was then applied to all APS-reported particle sizes for a given test. The expected sampling efficiency for each test aerosol was then calculated

$$\boldsymbol{\eta_i = \int[\eta(d_p) \cdot f_{m,i}(d_p)]dd_p} \quad (11)$$

where,

η_i = expected sampling efficiency for test aerosol i, and

$\eta(d_p)$ = modeled sampling efficiency for particles of size d_p, and

$f_{m,i}(d_p)$ = relative mass frequency of particles of size d_p in test aerosol i.

The modeled sampling efficiency for particles of size dp was calculated based on a Dagum distribution (Kleiber, 2008) sampling curve in this study:

$$\boldsymbol{\eta(d_p) = 1 - (1 + (\frac{d_p}{b})^{-a})^{-p}} \quad (12)$$

Where, a,b and p are adjustable coefficients to minimize SSE.

Where, a, b and p are parameters used to fit the curve. By default, lognormal distribution is the function to model FRM sampler. However, authors found Dagum distribution provided better fit of FRM sampler. In fact, according to Kolmogrov-Smirnov test, Dagum distribution perfectly fit FRM PM2.5 sampler.

With the expected sampling efficiency for each test particle defined, the sampling efficiency model was fit to the experimental data by adjusting a, b and p to minimize the SSE between observed effectiveness values and fitted curves. An iterative process was used because each change in the sampling effectiveness model resulted in changes to the expected sampling efficiency for a given test aerosol (Faulkner et al., 2014). Because the APS data accounts for satellites as well as multiplets, both artifacts are included in this correction.

After establishing the multiplets corrected curves based on Ranade and APS, as shown in Figure 7, the sampling efficiency at each particle size was determined, and the expected mass concentration that would be collected by the sampler when challenged with a given particle size distribution was calculated as:

$$\boldsymbol{C = \int [\eta(d_p) \cdot C(d_p)] dd_p} \quad (13)$$

Where,

C= expected mass concentration to be measured by the sampler ($\mu g/m^3$)

$\eta(dp)$ = sampling efficiency for particles of size dp,

C(dp) = mass concentration of particles of size dp in various particle size distributions described in Table 5 ($\mu g/m^3$).

RESULT AND DISCUSSIONS

Figure 7 shows the sampling effectiveness curves for both artifact correction methods using wind tunnel data. The sampling effectiveness curve using the Ranade method was obtained after 3 iterations and the SSE for was 1.01×10^{-02}. The SSE for APS correction method was 4.14×10^{-03}. The cutpoints were 2.57μm and 2.61 μm for the Ranade and APS methods, respectively. This represented a difference of 1.6% in the cutpoint between the methods. Based on equation 13, the mass concentration at different particle size distribution were calculated and shown in Table 5. The greatest difference of estimated sampled mass concentration was 0.3%.

Although the APS method provide a better fit both methods yielded satisfactory corrections. This was attributed to tuning the VOAG to eliminate satellites (Leong, 1986) during data collection.

However, the formation of satellites may occur during testing. In order to compare how the two methods responded with satellites present, an artificial data set was created assuming satellites and multiplets present at a mass fraction of 5% each.

The assumptions were: (1) the ideal FRM PM2.5 sampler modeled by the Dagum function was used to describe sampling effectiveness. (2) For each test, the mass fractions of singlets, doublets/triplets and satellites were 90%, 5%, and 5%, respectively,

as show in Table 6. (3) The Ranade method only took doublets and triplets into account (mass fraction of satellites was not used in this method).

Figure 8 shows the sampling effectiveness for the two artifact correction methods with satellites present. The APS method completely corrected for the presence of satellites. The corrected collection effectiveness at each particle size was the same as the ideal FRM sampler. The Ranade method was similar to the FRM at particle sizes smaller than 2.5um; however, when the particles were larger than 2.5um, the corrected collection efficiencies were greater than the FRM sampler efficiency curve. For example, the corrected sampling effectiveness at 3.5 μm was 9% while the FRM effectiveness was 0.5%. This was attributed to the large penetration effectiveness of the smaller satellite particles, which had an aerodynamic diameter from 1.6 to 2.0 μm. Since the Ranade method did not correct for satellites, the iterative curve fitting process was skewed, resulting in an overestimation of the penetration effectiveness for the larger diameter particles.

It turned out that, the FRM sampler used in calculation was no longer FRM sampler after Ranade method correction. The collection efficiencies on the right side of cutpoint (2.5 μm) were higher than FRM sampler since the Ranade method was not able to get rid of effect of the satellites.

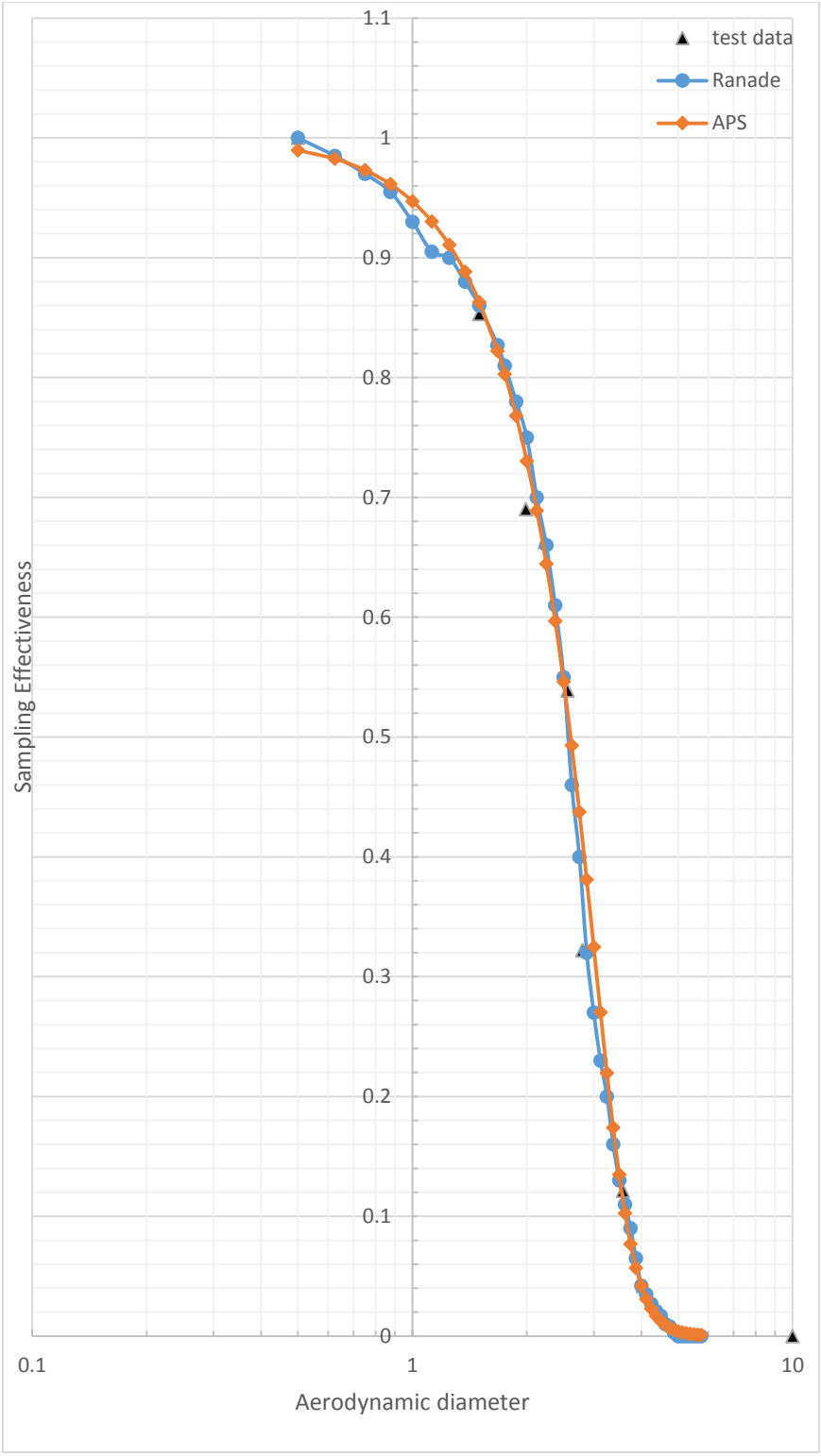

Figure 7. Multiplets corrected sampling effectiveness based on the Ranade and APS methods

Table 5. Cutpoint and mass concentration under 3 particle size distributions

		Ranade Method	APS method	Difference
Cutpoint (μm)		2.57	2.61	1.6%
Conc. (μg/m^3)	Coarse distribution[α]	14.366	14.415	0.3%
	"Typical" distribution[β]	34.206	34.154	-0.2%
	Fine distribution[γ]	75.683	75.745	0.1%

[α]Coarse distribution includes two modes, fine particle mode MMD=0.5μm, GSD=2 and Conc.=12.0 μg/m^3, and coarse particle mode MMD=10 μm, GSD=2 and Conc.= 88.0 μg/m^3

[β]"typical" distribution includes two modes, fine particle mode MMD=0.5μm, GSD=2 and Conc.=33.3 μg/m^3, and coarse particle mode MMD=10 μm, GSD=2 and Conc.= 66.7 μg/m^3

[γ]Fine distribution includes two modes, fine particle mode MMD=0.85 μm, GSD=2 and Conc.=85 μg/m^3, and coarse particle mode MMD=15 μm, GSD=2 and Conc.= 15 μg/m^3.

Table 6. Particle size distribution

AED (um)	Test 1	Test 2	Test 3	Test 4	Test 5	Test 6	Test 7
1.5	90%						
1.6							
1.7			1%	1%		1%	1%
1.8	5%		3%	3%		3%	3%
2.0		90%		1%	1%	1%	1%
2.1					3%		
2.3	1%		90%		1%		
2.5	3%	4%	1%	90%			
2.6	1%						
2.8		1%	5%		90%		
3.1				5%			
3.3							
3.5		1%			5%	90%	
3.8		3%					
4.1		1%					90%
4.4						5%	
4.7							
5.0							5%

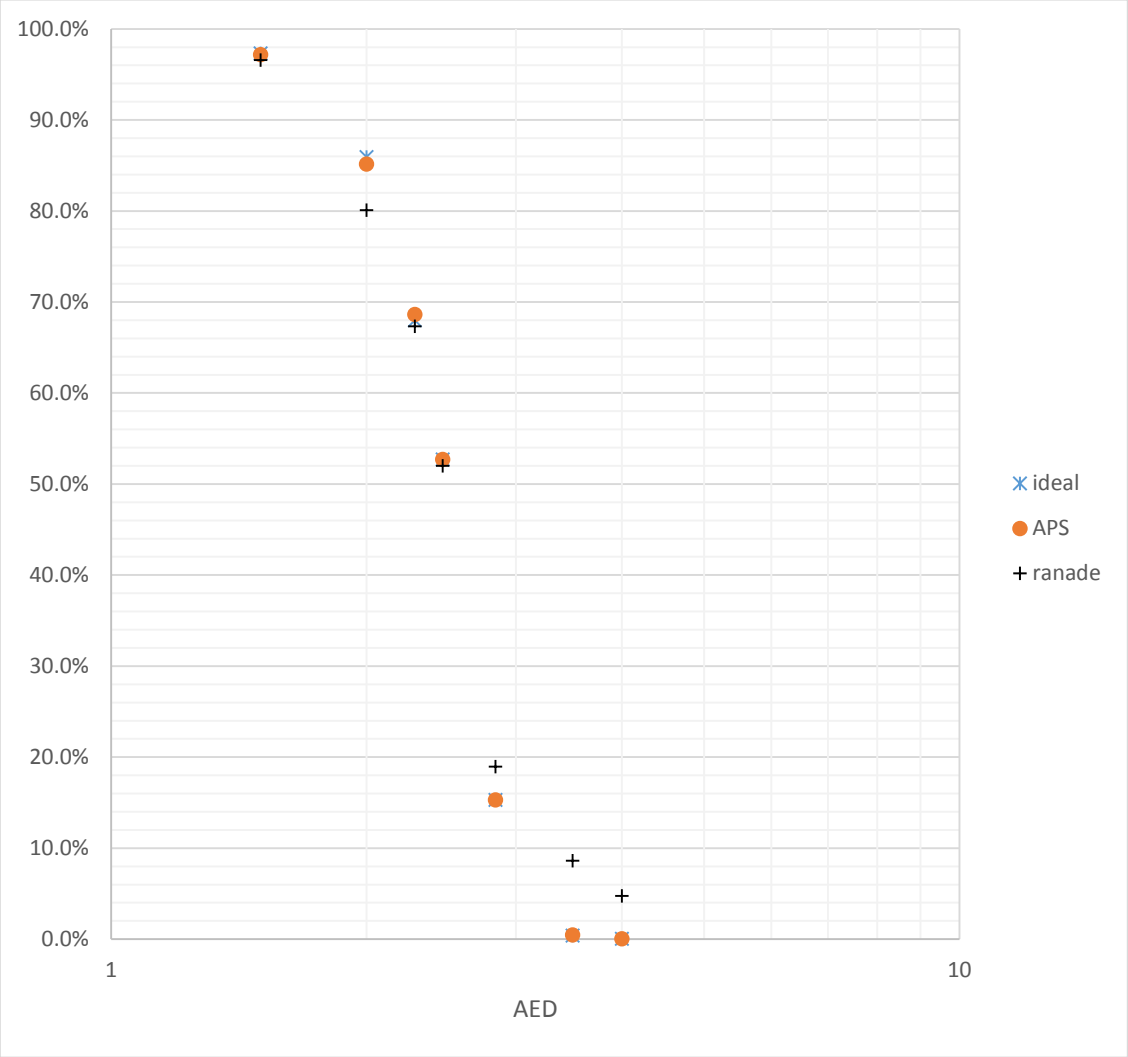

Figure 8. Collection effectiveness of ideal FRM PM2.5 sampler and effectiveness corrected by Ranade and APS methods

CONCLUSIONS

A PM2.5 sampler was challenged by monodisperse aerosols generated by VOAG in a wind tunnel under controlled conditions. Methods based on Ranade (1990) and APS data (Haglund et al., 2002) were used to perform to correct the data for multiplets to

obtain a sampling effectiveness curve. Because the VOAG was tightly controlled, satellites were not present in these data. Both methods satisfactorily corrected for the effect of multiplets. The cutpoint of the corrected sampling effectiveness curve based on APS data was 2.61 μm and the difference between two methods was 1.6%. Mass concentrations based on 3 different PSDs were calculated and the greatest difference of estimated sampled mass concentration was 0.3%.

Theoretical calculations were performed to determine how the two methods performed with satellites present in the data at a mass fraction of 5%. The APS method corrected for the effect of satellites, while the Ranade method was sensitive to the satellites, resulting in an overestimated of sampling effectiveness at larger particle sizes (> 2.5 μm).

Therefore, when the VOAG was finely tuned, both methods could effectively correct for doublets and triplets. However, when there were satellites, the Ranade method did not effectively correct the penetration effectiveness cure. The APS methods is recommended in this situation.

The data from wind tunnel tests are time consuming and high cost. It would be beneficial if the data with satellites can be used. APS method is able to correct artifacts in monodisperse aerosols generated by VOAG, and this method is able to utilize the test data with satellites, which Ranade method must reject.

In order to perform Ranade method, at least 100 particle diameter measurements by optical microscope are required. This method is also based on hand-drawn curves, which may introduce other potential error. This hand-drawn process must be repeated at

least 3 times to get a stable curve and is more time consuming than APS method, which is based on equations 3-6 and mass fraction measured by APS and can be easily processed by computer. However, the cost of APS is non-trivial and may limit its implementation.

CHAPTER IV

SELECTION OF DISTRIBUTION FUNCTIONS TO MODEL FEDERAL REFERENCE METHOD SAMPLER DATA

OVERVIEW

The lognormal distribution is widely used in the theoretical calculation and modeling of PM samplers; however, this paper demonstrates that the error resulting from the lack of fit of the lognormal distribution is non-trivial. The error can be as high as 22.68% with the lognormal distribution. Ten distribution functions were applied to fit the performance curve given for FRM PM2.5 and PM10 samplers. The Kolmogorov Smirnov test and mass concentration calculation determined that the Dagum distribution provided the best fit among the ten functions. In order to achieve a high goodness of fit and a low mass concentration error, the Dagum distribution is recommended for theoretical calculations of FRM PM samplers.

Keywords: FRM, PM2.5, PM10, best fit, Dagum distribution, lognormal distribution

INTRODUCTION

The National Ambient Air Quality Standards (NAAQS) are the basis for the U.S. Environmental Protection Agency (EPA) to regulate pollutants, including particulate matter (PM) and five others. PM with aerodynamic diameter (AED) less than 2.5μm and 10 μm is currently two indicators for PM pollutions (PM2.5 and PM10). The mass concentration of PM2.5 and PM10 in ambient air are measured by the EPA-approved

Federal Reference Method (FRM) or Federal Equivalent Method (FEM) PM2.5 and PM10 samplers.

The lognormal distribution function is widely used in theoretical calculation and modeling of FRM PM samplers. This function is applied to describe not only the performance of PM2.5 and PM10 sampler, but also particle size distributions (Buser et al. 2001; 2007; Buser et al. 2008; Faulkner et al. 2007; Capareda et al. 2004).

Although there is no fundamental theoretical reason why particle size data should approximate the lognormal distribution, it has been found to apply to most single-source aerosols (Hinds 2012). The lognormal mass density function for particle size distribution is expressed as:

$$\boldsymbol{f(d_p, MMD, GSD)} = \frac{1}{d_p \ln(GSD)\sqrt{2\pi}} \exp\left[\frac{-(\ln(d_p)-\ln(MMD))^2}{2[\ln(GSD)]^2}\right] \qquad (14)$$

where,

d_p is the aerodynamics diameter of particle (μm),

MMD is the mass median diameter (μm),

GSD is the geometric standard deviation.

When it comes to performance of the PM sampler, the lognormal distribution is the default function to describe sampler performance because its arithmetic mean (μ) and geometric standard deviation (σ) instinctively describe the two key parameters of PM sampler performance: cutpoint and sharpness (or slope). The lognormal density distribution function for sampling effectiveness of the FRM sampler is defined as:

$$\boldsymbol{\varepsilon(d_p, d_{50}, slope)} = 1 - \frac{1}{d_p \ln(slope)\sqrt{2\pi}} \exp\left[\frac{-(\ln(d_p)-\ln(d_{50}))^2}{2[\ln(slope)]^2}\right] \qquad (15)$$

where,

d50 (also referred as the cutpoint) is the particle size where 50% of the PM is captured by the pre-separator and 50% of the PM penetrates to the filter;

slope is the ratio of the particle sizes corresponding to cumulative sampling effectiveness of 84.1% and 50% (d84.1/d50) or 50% and 15.9% (d50/d15.9).

If the slope is equal to 1 (i.e. the sampler is perfectly sharp), the sampling effectiveness curve of PM2.5 or PM10 sampler can be described as a step function, which means 100% sampling effectiveness for particles with AED<2.5/10 μm, and 0% sampling effectiveness for particles with AED>2.5/10 μm. However, from an engineering standpoint it is not possible to design a sampler with slope of 1. The slope of the sampling effectiveness curve is always greater than 1 for any practical PM sampler based on impaction theory.

The d50 values for both FRM PM2.5 and PM10 samplers are explicitly stated in the EPA standards as 10.0± 0.5 μm and 2.5 ± 0.2 μm, respectively. No slope values for the sampler are listed in EPA's 40 CFR Part 53; however, idealized sampler performance curves in tabular form are available and the sampler performance slope can be calculated (Table D3 of subpart D and Table F4 of Subpart F of Part 53, 40 CFR).

Ideally, the performance curve can be fit to a cumulative lognormal distribution with appropriate d50 and slope; however, it was found that no single cumulative lognormal curve adequately represented the EPA idealized sampler performance curves (Buser et al. 2003). To simplify the process, the performance of FRM PM2.5 sampler has been described as a lognormal distribution with d50 of 2.5 ± 0.2 μm and slope of

1.18 (Peters and Vanderpool 1996) or 1.3 ± 0.03 (Buch 1999). The performance of the FRM PM10 sampler has been described with d50 of 10.0 ± 0.5 μm and slope of 1.5 ± 0.1(Buser et al. 2001).

The objectives of this study were to quantify the error arising from the application of the lognormal distribution to the performance curve of the FRM PM2.5 and PM10 samplers and to evaluate other continuous distribution functions to determine if a better fit is achievable.

METHODOLOGY

Distribution functions

Ten distribution functions including the lognormal function (Table 7) were fit to the performance curves for the FRM PM2.5 and PM10 samplers. The sum of squared error between the value of distribution function and table data was minimized by adjusting the coefficients of each function.

The sum of squared error (SSE) was calculated as:

$$\boldsymbol{SSE} = \sum(\boldsymbol{E_i} - \boldsymbol{\eta_i})^{\boldsymbol{2}} \tag{16}$$

where,

Ei is sampling effectiveness calculated by the distribution function for particle size i, and

η_i is the ideal sampling effectiveness from 40 CFR Part 53 tabular for particle size i.

Microsoft Excel® was used to adjust the coefficients of each distribution function to minimize the SSE. Once the minimized SSE was achieved, the coefficients

were determined and the sampling effectiveness for each function at different particle sizes was determined. Six particle size distributions (Table 8 and Table 9) were used in these calculations. The mass concentrations for different particle size distributions were calculated based on equation 17 and compared with the concentrations based on the ideal FRM PM2.5 and PM10 samplers.

$$\boldsymbol{C_i = \int_0^i p(x) \cdot f(x) dx} \quad (17)$$

where,

C_i is mass concentration of PM smaller than or equal to size i,

i is indictor size (2.5 μm fro PM2.5 and 10 μm for PM10)

p(x) is cumulative distribution function that fits the FRM sampler,

f(x) is particle size distribution of dust.

Error of mass concentration was determined by equation 18:

$$\boldsymbol{error = \frac{(mass\ conc.of\ distribution\ fucntion - mass\ conc.of\ ideal\ sapmler)}{mass\ conc.of\ ideal\ sampler} \times 100\%} \quad (18)$$

Test of goodness of fit

The Kolmogorov Smirnov test (K-S test) was used as the goodness of fit criterion (Lu and Fang 2003). Each distribution function was compared with the ideal performance curve and the K-S test calculated the largest absolute difference (Dmax) between the two distributions. Dmax was used with the K-S probability function to calculate the probability value (p). A smaller Dmax indicates a better goodness of fit and as the p value approaches 1 the distributions are more similar. The K-S test results were used to determine the distribution function that provided the best fit to the ideal FRM

PM2.5 and PM10 sampler performance. Detailed calculations are available on Table 12 to 15.

RESULTS AND DISCUSSIONS

The cumulative distribution functions used to fit FRM sampler and their SSEs are listed Table 7. When compared to the lognormal distribution, five distribution functions fit with lower SSE for the PM2.5 sampler; while all distribution functions, except for the Fréchet distribution, fit with lower SSE for the PM10 sampler. For both FRM PM2.5 and PM10 samplers, the SSEs of Dagum distribution were the lowest, where a=18.43, b=2.78, c=0.31 for the PM2.5 sampler and a=42.20, b=15.51, c=0.04 for the PM10 sampler, respectively. Figure 9 and Figure 10 show the Dagum and lognormal distributions and provide graphical demonstration of the better fit.

For the PM2.5 sampler, p = 1 for the Dagum and Weibull distribution; and for the PM10 sampler, p = 0.999 for the Dagum distribution. When p is equal to 1 the two distributions evaluated by the K-S test are the same, which means that Dagum distribution perfectly fit the FRM PM2.5 sampler and was almost a perfect fit for the FRM PM10 sampler. The corresponding p values for the best-fit lognormal distribution were p = 0.58 and p = 0.111 for the PM2.5 and PM10 samplers, respectively.

Table 7. Cumulative distribution functions, SSEs and p-values to fit performance of the ideal FRM PM2.5 and PM10 samplers

Cumulative distribution function	Mathematical description	coefficients	PM2.5			PM10		
			SSE	Dmax	p	SSE	Dmax	p
Dagum distribution(Kleiber 2008)	$(1+(\frac{x}{b})^{-a})^{-c}$	a, b, c	2.95E-04	0.0698	1	5.95E-03	0.0811	0.999
Weibull Distribution(Evans et al. 2000)	$1-e^{-\left(\frac{x}{\lambda}\right)^{k}}, for\ x \geq 0$	λ, k	6.10E-04	0.0698	1	5.54E-02	0.1622	0.676
Logistic distribution(Balakrishnan 2013)	$\frac{1}{1+e^{-\frac{x-\mu}{s}}}$	μ, s	5.62E-03	0.1395	0.765	3.90E-02	0.2162	0.314
Folded normal distribution(Leone et al. 1961)	$\frac{1}{2}[\mathrm{erf}\left(\frac{x+\mu}{\sigma\sqrt{2}}\right) + \mathrm{erf}(\frac{x-\mu}{\sigma\sqrt{2}})]$	μ, σ	5.80E-03	0.1163	0.917	3.78E-02	0.1622	0.676
Gamma distribution(Stacy 1962)	$\frac{\gamma(\alpha,\beta x)}{\Gamma(\alpha)}$	α, β	1.26E-02	0.1395	0.765	9.95E-02	0.2432	0.193
Lognormal distribution(Aitchison and Brown 1976)	$\frac{1}{2}+\frac{1}{2}\mathrm{erf}[\frac{\ln(x)-\mu}{\sigma\sqrt{2}}]$	μ, σ	1.69E-02	0.1628	0.580	1.35E-01	0.2703	0.111

Table 7. Continued

Cumulative distribution function	Mathematical description	coefficients	PM2.5			PM10		
			SSE	Dmax	p	SSE	Dmax	p
Log-logistic distribution(Bennett 1983)	$\frac{1}{1+(x/\alpha)^{-\beta}}$	α, β	1.69E-02	0.2791	0.2791	1.33E-01	0.2162	0.314
Gumbel distribution(Nadarajah and Kotz 2004)	$e^{-e^{-(x-\mu)/\beta}}$	μ, β	3.51E-02	0.2326	0.169	1.10E-01	0.2703	0.111
Shifted gompertz distribution(Bemmaor 1992)	$(1-e^{-bx})e^{-\eta e^{-bx}}$	b,η	3.51E-02	0.2326	0.169	1.12E-01	0.2703	0.111
Fréchet distribution(de Gusmão et al. 2011)	$e^{-(\frac{x-m}{s})^{-\alpha}}$	m, s, α	5.57E-02	0.4186	0.001	2.41E-01	0.3243	0.031

Table 8 lists calculated PM2.5 concentrations and errors based on different distribution functions for five particle size distributions and Table 9 lists calculated PM10 Concentrations and errors based on different distribution functions for three particle size distributions. For the FRM PM2.5 sampler with a lognormal distribution function (d50=2.5 μm and slope =1.3) the error from the lack of fit of the lognormal function was as high as 22.68%. The reason for such large error was the large sampling effectiveness for particles in the range from 2.5 to 5 μm as shown in Figure 9. For the FRM PM10 sampler, the mass concentration error of best-fit lognormal distribution (d50 = 9.8 μm and slope = 1.52) was less than the default lognormal distribution (d50 = 10.0 μm and slope = 1.50); however, it was still significantly larger than the errors for the Weibull and Dagum distributions.

Table 8. Calculated PM2.5 Concentrations and errors based on different distribution functions with five particle size distributions

		Coarse[1]	"Typical"[2]	Fine[3]	urban PM[4]	agricultural PM[5]
Ideal (Table F4 of Subpart F of Part 53, 40 CFR)	Conc.(μg/m^3)	13.814	34.284	78.539	28.125	10.575
Lognormal (best fit, d50=2.44μm,slope=1.18)	Conc. (μg/m^3)	13.944	34.459	79.193	28.899	10.949
	error	0.94%	0.51%	0.83%	2.75%	3.53%
Lognormal (d50=2.5 μm, slope=1.3)	Conc.(μg/m^3)	14.519	34.796	78.894	31.703	12.974
	error	5.10%	1.49%	0.45%	12.72%	22.68%
Weibull distribution	Conc.(μg/m^3)	13.834	34.331	78.760	28.200	10.596
	error	0.14%	0.14%	0.28%	0.27%	0.19%
Dagum distribution	Conc.(μg/m^3)	13.833	34.311	78.619	28.183	10.613
	error	0.14%	0.08%	0.10%	0.21%	0.36%
Log-logistic distribution	Conc.(μg/m^3)	13.983	34.476	79.150	29.068	11.086
	error	1.22%	0.56%	0.78%	3.35%	4.83%
Gamma distribution	Conc.(μg/m^3)	13.925	34.440	79.132	28.779	10.886
	error	0.80%	0.45%	0.76%	2.32%	2.94%
Folded normal distribution	Conc.(μg/m^3)	13.889	34.398	78.986	28.543	10.769
	error	0.54%	0.33%	0.57%	1.48%	1.83%

[1] Coarse distribution includes two particle modes, fine particle mode with MMD=0.5μm, GSD=2 and Conc.=12.0 μg/m^3, coarse particle mode with MMD=10 μm, GSD=2 and Conc.= 88.0 μg/m^3.

[2] "Typical" distribution includes two particle modes, fine particle mode with MMD=0.5 μm, GSD=2 and Conc.=33.3 μg/m^3, coarse particle mode with MMD=10 μm, GSD=2 and Conc.= 66.7 μg/m^3.

[3] Fine distribution includes two particle modes, fine particle mode with MMD=0.85 μm, GSD=2 and Conc.=85 μg/m^3, coarse particle mode with MMD=15 μm, GSD=2 and Conc.= 15 μg/m^3.

[4] urban PM with MMD=5.7 μm, GSD=2.25 and Conc. =198.44 μg/m^3

[5] agricultural PM with MMD=15 μm, GSD=2.5 and Conc. =455.84 μg/m^3

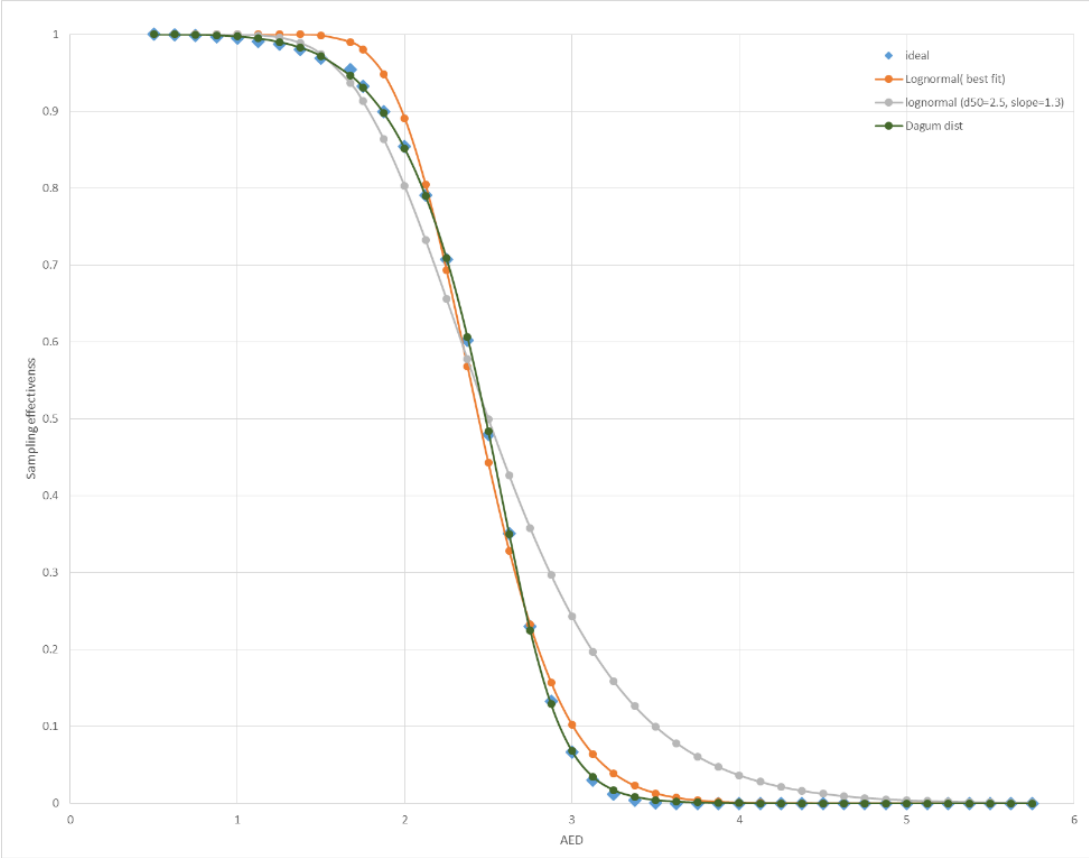

Figure 9. Lognormal and Dagum distribution fits for FRM PM2.5 sampler

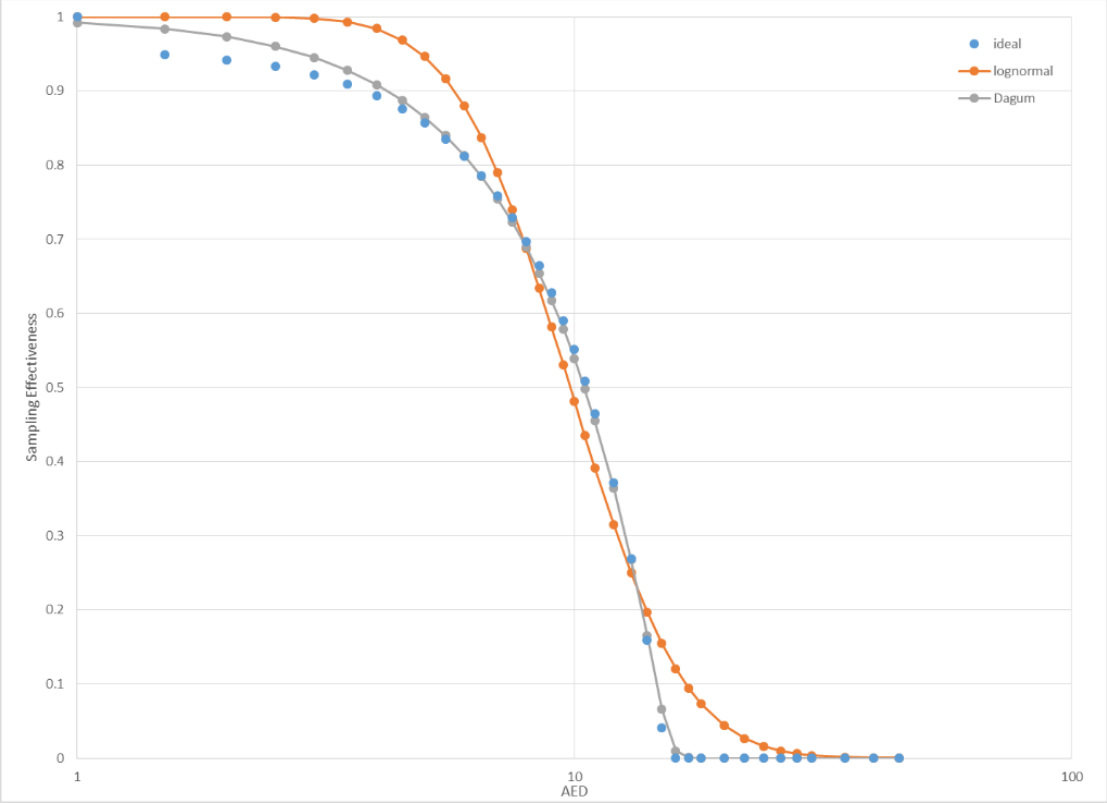

Figure 10. Lognormal and Dagum distribution fits for FRM PM10 sampler (x-axis in logarithmic scale to highlight the difference)

Table 9. Calculated PM10 Concentrations and errors based on different distribution functions with three particle size distributions

		PM[6]	urban PM	Agricultural PM
Ideal (Table D3 of Subpart D of Part 53, 40 CFR)	Conc.(μg/m^3)	143.890	132.845	138.012
Lognormal (d50=10 μm, slope=1.5)	Conc.(μg/m^3)	150.646	142.699	150.464
	error	4.70%	7.42%	9.02%
Lognormal (best fit, d50=9.8 μm, slope=1.52)	Conc.(μg/m^3)	148.940	140.976	147.610
	error	3.51%	6.12%	6.95%
Weibull distribution	Conc.(μg/m^3)	146.460	137.835	142.890
	error	0.71%	0.78%	0.75%
Dagum distribution	Conc.(μg/m^3)	143.847	134.268	138.620
	error	-0.03%	1.07%	0.44%
Logistic distribution	Conc.(μg/m^3)	144.690	135.511	142.427
	error	0.56%	2.01%	3.20%
Folded normal distribution	Conc.(μg/m^3)	145.261	135.808	141.732
	error	0.95%	2.23%	2.70%
Gamma distribution	Conc.(μg/m^3)	147.909	139.377	145.468
	error	2.79%	4.92%	5.40%

[6] Particle size distribution is available on Table D, 40 CFR part 53 subpart D.

Buser et al. (2001) did theoretical calculation of PM10 and PM2.5 sampler with lognormal distribution. For PM with MMD = 20 μm, GSD = 2.0 and PM10 concentration of 150 μg/m^3, the theoretical PM10 concentration with lognormal distribution (d50 = 10.0 μm and slope = 1.50) is 183.5 μg/m^3; based on equation 17 and Table 9, calculated PM10 concentration by Dagum distribution can be determined, 152.7 μg/m^3. The imparity between the true PM10 concentration (150 μg/m^3) and calculated PM10 concentration (183.5 μg/m^3 or 152.7 μg/m^3) is called oversampling (Capareda et al. 2004). The concentration error by the performance of sampler is 2.7 μg/m^3, while the concentration error by the lognormal function fit is 30.8 μg/m^3. The lognormal function fit error is 11.4 times higher than error from sampler performance. From this calculation, it is clear that lognormal function fit error overweighs error from sampler. Although oversampling was found commonly in agricultural operations experimentally and theoretically, it is overstated due to lognormal distribution fit in theoretical calculation.

CONCLUSIONS

The lognormal distribution is widely used in the theoretical calculation and modeling of PM sampler; however, the lack of fit from the lognormal distribution is non-trivial and was shown to be as large as 22.68%. The Dagum distribution was found to provide a better fit for the FRM PM2.5 and PM10 samplers. Based on mass concentration calculations using the Dagum distribution for a variety of particle size distributions, the error was demonstrated to be in the range of -0.03% to 1.07%. Because of the improved goodness of fit and small mass concentration errors, the Dagum distribution is recommended to be used to model the FRM PM2.5 and PM10 samplers.

CHAPTER V

PM2.5 EMISSION FACTORS FOR AGRICULTURAL OPERATIONS

OVERVIEW

The PM2.5 emission factors for agricultural operations, such as cattle feed yard, dairies, cotton gins et al., were determined in this study. The method is based on the TSP concentration and particle size distribution data from Center for Agricultural Air Quality Engineering and Science.

Keyword: PM2.5, emission factor, agricultural operations

INTRODUCTION

Air pollutions are any solid, liquid, or gas that is present in the air in a concentration that causes some deleterious effect. Exposure to air pollutions has been associated with increases in mortality and hospital admissions due to respiratory and cardiovascular disease. These effects have been found in short-term and long-term studies (Brunekreef and Holgate, 2002). Exposure to fine particulate has been associated with lung cancer, and cardiopulmonary mortality. Each 10 $\mu g/m^3$ elevation in fine particulate air pollution was associated with approximately a 6%, and 8% increased risk of cardiopulmonary, and lung cancer mortality, respectively (Pope III et al., 2002).

In order to protect public health and welfare, the National Ambient Air Quality Standards (NAAQS) have been established for six criteria air pollutions: five primary and one secondary pollutant (Cooper and Alley, 2002). One of the five primary

pollutants is particle pollution, which includes two indicators, particulate matter with aerodynamic diameter less than 10 μm (PM10), and particulate matter with aerodynamic diameter less than 2.5 μm (PM2.5).

The PM10 limit was a 24-hour concentration of 150 $\mu g/m^3$. The PM2.5 24-hour NAAQS was initially set at 65 $\mu g/m^3$ and was revised to 35 $\mu g/m^3$ and an annual NAAQS of 12 $\mu g/m^3$.

The U.S. EPA defines an emission factor (USEPA, 2000) as: An emissions factor is a representative value that attempts to relate the quantity of a pollutant released to the atmosphere with an activity associated with the release of that pollutant. These factors are usually expressed as the weight of pollutant divided by a unit weight, volume, distance, or duration of the activity emitting the pollutant (e.g., kilograms of particulate emitted per megagram of coal burned). Such factors facilitate estimation of emissions from various sources of air pollution. In most cases, these factors are simply averages of all available data of acceptable quality, and are generally assumed to be representative of long-term averages for all facilities in the source category (i.e., a population average).

The general equation for emission estimation is:

$$E = A \times EF \times (1 - ER/100) \tag{19}$$

where:

E = emissions;

A = activity rate;

EF = emission factor, and

ER =overall emission reduction efficiency, %

The advantage of emission factor is that emissions calculation can easily be scaled up or down as the facility activities vary. An emission factor is expressed in terms of mass per production unit and is calculated from an emission rate. (Lacey et al., 2003).

The purpose of this objective is to calculate the PM2.5 emission factor for feed mills, cattle feed yards, dairies, cotton gins, and grain elevators using TSP concentration and particle size distribution data from Center for Agricultural Air Quality Engineering and Science.

The purpose of this research is to determine science based emission factor for PM2.5 permitting and to minimize the impact on agricultural operations of moving to permitting based upon PM2.5 emissions and PM2.5 NAAQS compliance.

METHODOLOGY

The center for agricultural air quality engineering and science (CAAQES) has an extensive database of measured PM concentrations and have published emission factors for cotton gins, feed mills, cattle feed yards, grain elevators, and dairies. This database is the most extensive in existence of its kind and includes upwind and downwind concentrations over various periods of time over two decades. This database was used to determine PM2.5 emission factors.

The terminology of “True PM10 or “True PM2.5” are used in Air Quality (AQ) work performed in CAAQES. This work is typically associated with “permitting” and/or “research” to determine emission factors of agricultural facilities. Particulate matter emitted from point and fugitive agricultural sources are often characterized as large

compared to PM associated with urban PM. PM can be characterized as lognormal with a mass median diameter (MMD) and geometric standard deviation (GSD). Agricultural PM typically has an MMD equal to 20 micrometers (μm) and a GSD equal to 2. Whereas Urban PM will typically have an MMD=5 and a GSD=1.5 (Sweeten et al., 1998).

True PM2.5 is the mass fraction of the mass less than 2.5 μm obtained from a particle size distribution of PM captured with a TSP sampler, times the measured TSP concentration. There are 3 main steps to determine the true PM2.5:

(1) Gravimetrically determine the mass concentrations of TSP using Low-Vol TSP (LVTSP) sampler.

(2) Determine the particle size distribution (PSD) of collected PM on the LVTSP filter using Coulter counter analysis. This consists of counting and sizing approximately 300,000 particles that could range in size from 2.3 μm to 100 μm aerodynamic diameter. The ratio of d84.1/d50 is the GSD and the d50 is the MMD.

(3) The resulting PSD can be used to determine the percent mass of PM2.5 of the PM. By multiplying the percent mass of PM2.5 times the measured concentration, one can approximate the true concentration PM2.5 (Buser et al., 2007).

Based on this method, the PM2.5 emission factor for agricultural operation were determined based on the CAAQES database, as shown in Table 10.

Table 10. PM10 and PM2.5 Emission factors for agricultural operation

Ag operation	TSP	MMD (μm)	GSD	PM10 fraction	PM2.5 fraction	PM10	PM2.5
Cattle feed yard(Wanjura et al., 2004)	8.1kg/(1000hd*day)	17.4	2.2	24.1%	0.7%	2 kg/(1000hd*day) .	0.06 kg/(1000hd*day).
Dairies (Goodrich et al., 2002)	8.1kg/(1000hd*day)	17.4	2.2	24.1%	0.7%	2 kg/(1000hd*day)	0.06 kg/(1000hd*day)
Cotton Gins(Buser et al., 2008)	3.1 lb/bale	15.2	2.11	28.7%	0.8%	0.881 lb/bale	0.0246 lb/bale
Feed mills(Shaw et al., 1998)	0.3lbs/ton	\	\	15% 25%(EPA)	0.2-1%	3 g/tonne for unloading grain 1.0 g/tonne for loading feed	0.2 g/tonne for unloading grain 0.025 g/tonne for loading feed
Grain elevators (Parnell, 1994)	0.3 lbs/ton	\	\	15% 25%(EPA)	0.2-1%	3 g/tonne for unloading grain 1.0 g/tonne for loading feed	0.2 g/tonne for unloading grain 0.025 g/tonne for loading feed

CONCLUSIONS

The PM2.5 emission factors for agricultural operations were determined, based on the TSP concentration and particle size distribution data from Center for Agricultural Air Quality Engineering and Science.

CHAPTER VI

GENERAL CONCLUSIONS

SUMMARY

Two sets of nozzles were tested in a sampler that was placed in a wind tunnel, and penetration efficiencies, $\sqrt{Stk_{50}}$ and slope of the performance curve were determined by fluorometric analysis. It was shown that even small changes in nozzle geometry that require the simplest changes in tooling can significantly affect impactor performance. While the key parameter, inner diameter, remained the same, small changes in convergence angle significantly affected Stk_{50} and slope of the performance curve, less aggressive convergence angle can reduce the crossing trajectory phenomenon, thus improving the impactor performance for (i.e., reducing penetration of) particles larger than the cut point. After modification, the $\sqrt{Stk_{50}}$ of the nozzle decreased to 0.49, which is the same for a well-designed impactor, regardless of the nozzle diameter or velocity.

A PM2.5 sampler was challenged by monodisperse aerosols generated by VOAG in a wind tunnel under controlled conditions. Methods based on Ranade and APS data were used to perform the multiplets correction to get corrected sampling effectiveness curve for PM2.5 sampler. Mass concentrations based on 3 kinds of particle size distributions were calculated. Theoretical calculations were also performed to study how the two methods respond under satellites with mass fraction of 5%. In the wind tunnel tests, where the test condition were tuned to eliminate the satellites, both methods corrected the effect of doublets/triplets and yielded similar results. The cutpoint of the corrected sampling effectiveness curve based on APS data was 2.61 μm, the difference

between two methods is 1.6%, and highest difference of mass concentration is only 0.3%. In theoretical calculations, the APS method completely corrected the effect of satellites since APS provided all particle size distribution data; however, the Ranade method was determined to be sensitive to the satellites, especially for the larger particle where the collection effectiveness was low. When the VOAG is finely tuned and aerosol is monodisperse, both methods can effectively correct doublets and triplets. However, when there are satellites, even as low as 5%, these satellites have significant effect on Ranade method. APS methods is recommended to use in this situation.

The lognormal distribution is widely used in the theoretical calculation and modeling of PM sampler; however, the lack of fit from the lognormal distribution is non-trivial and was shown to be as large as 22.68%. The Dagum distribution was found to provide a better fit for the FRM PM2.5 and PM10 samplers. Based on mass concentration calculations using the Dagum distribution for a variety of particle size distributions, the error was demonstrated to be in the range of -0.03% to 1.07%. Because of the improved goodness of fit and small mass concentration errors, the Dagum distribution is recommended to be used to model the FRM PM2.5 and PM10 samplers.

The PM2.5 emission factors for agricultural operations were estimated based on the TSP concentration and particle size distribution data from Center for Agricultural Air Quality Engineering and Science.

RECOMMENDATIONS FOR FUTURE RESEARCH

The goal of the second objective was to eliminate the artifacts created in the production of a monodisperse aerosol by VOAG. However, a better understanding of mechanism of transition from monodisperse to polydisperse aerosol is necessary. The current governing equation of VOAG (Berglund and Liu, 1973) is not able to explain this transition.

The p value for Dagum distribution to fit FRM PM10 is 0.999, which is quite close to 1. However, there is still a chance to find better distribution function to fit the FRM PM10 sampler.

REFERENCES

Aitchison, J., and J. A. C. Brown. 1976. The lognormal distribution. CUP Archive.

Balakrishnan, N. 2013. Handbook of the logistic distribution. CRC Press.

Baron, P. A. 1986. Calibration and use of the aerodynamic particle sizer (APS 3300). Aerosol Science and Technology 5(1):55-67.

Bemmaor, A. C. 1992. Modeling the diffusion of new durable goods: Word-of-mouth effect versus consumer heterogeneity. In Research traditions in marketing, 201-229. Springer.

Bennett, S. 1983. Log-logistic regression models for survival data. Applied Statistics 32(2):165-171.

Berglund, R. N., and B. Y. H. Liu. 1973. Generation of monodisperse aerosol standards. Environmental Science & Technology 7(2):147-153.

Brunekreef, B., and S. T. Holgate. 2002. Air pollution and health. The Lancet 360(9341):1233-1242.

Buch, U. 1999. Performance analysis of the cascade impactor, the federal reference method PM2. 5 sampler and the IMPROVE sampler. Master of Science Thesis. Department of Agricultural Engineering, Texas A&M University, College Station, Texas.

Buser, M., C. Parnell, B. Shaw, and R. Lacey. 2007. Particulate matter sampler errors due to the interaction of particle size and sampler performance characteristics: background and theory. Transactions of the ASABE 50(1):221-228.

Buser, M. D., C. B. Parnell, R. E. Lacey, B. W. Shaw, and B. W. Auvermann. 2001. Inherent biases of PM10 and PM2. 5 samplers based on the interaction of particle size and sampler performance characteristics. In 2001 ASAE Annual Meeting. American Society of Agricultural and Biological Engineers.

Buser, M. D., J. D. Wanjura, D. P. Whitelock, S. C. Capareda, B. W. Shaw, and R. Lacey. 2008. Estimating FRM PM10 sampler performance characteristics using particle size analysis and collocated TSP and PM10 samplers: cotton gins. Transactions of the ASABE 51(2):695-702.

Capareda, S., L. Wang, C. Parnell Jr, and B. Shaw. 2004. Particle size distribution of particulate matter emitted by agricultural operations: Impacts on FRM PM10

and PM2. 5 concentration measurements. In Proc. of the 2004 Beltwide Cotton Production Conferences, National Cotton Council, Memphis, Tenn.

Cooper, C. D., and F. C. Alley. 2002. Air pollution control: A design approach. Waveland Press.

de Gusmão, F. R., E. M. Ortega, and G. M. Cordeiro. 2011. The generalized inverse Weibull distribution. Statistical Papers 52(3):591-619.

Evans, M., N. Hastings, and B. Peacock. 2000. Statistical distributions.

Faulkner, W., B. Shaw, and R. Lacey. 2007. Coarse fraction aerosol particles: Theoretical analysis of rural versus urban environments. Applied Engineering in Agriculture 23(2):239-244.

Faulkner, W. B., and J. S. Haglund. 2012. Flattening coefficients for oleic acid droplets on treated glass slides. Aerosol Science and Technology 46(7):828-832.

Faulkner, W. B., R. Smith, and J. Haglund. 2014. Large particle penetration during PM10 sampling. Aerosol Science and Technology 48(6):676-687.

Goodrich, L., C. Parnell, S. Mukhtar, R. Lacey, and B. Shaw. 2002. Preliminary PM10 emission factor for freestall dairies. In ASAE Annual International Meeting/CIGR XVth World Congress.

Haglund, J. S., S. Chandra, and A. R. McFarland. 2002. Evaluation of a high volume aerosol concentrator. Aerosol Science and Technology 36(6):690-696.

Hari, S., A. R. McFarland, and Y. A. Hassan. 2007. CFD study on the effects of the large particle crossing trajectory phenomenon on virtual impactor performance. Aerosol Science and Technology 41(11):1040-1048.

Hillamo, R. E., and E. I. Kauppinen. 1991. On the performance of the Berner low pressure impactor. Aerosol Science and Technology 14(1):33-47.

Hinds, W. C. 2012. Aerosol technology: properties, behavior, and measurement of airborne particles. John Wiley & Sons.

John, W. 1999. A simple derivation of the cutpoint of an impactor. Journal of Aerosol Science 30(10):1317-1320.

Jurcik, B., and H.-C. Wang. 1995. On the shape of impactor efficiency curves. Journal of Aerosol Science 26(7):1139-1147.

Kleiber, C. 2008. A guide to the Dagum distributions. In Modeling Income Distributions and Lorenz Curves, 97-117. Springer.

Leone, F., L. Nelson, and R. Nottingham. 1961. The folded normal distribution. Technometrics 3(4):543-550.

Leong, K. 1986. On the continuous operation of the vibrating orifice aerosol generator. Journal of Aerosol Science 17(5):855-858.

Li, H. 2013. Performance of a high volume PM2. 5 sampler. Texas A&M University,

Lu, H.-C., and G.-C. Fang. 2003. Predicting the exceedances of a critical PM 10 concentration—a case study in Taiwan. Atmospheric Environment 37(25):3491-3499.

Marjamäki, M., J. Keskinen, D.-R. Chen, and D. Y. Pui. 2000. Performance evaluation of the electrical low-pressure impactor (ELPI). Journal of Aerosol Science 31(2):249-261.

Marple, V. A., K. L. Rubow, W. Turner, and J. D. Spengler. 1987. Low flow rate sharp cut impactors for indoor air sampling: design and calibration. Japca 37(11):1303-1307.

Marple, V. A., and K. Willeke. 1976. Impactor design. Atmospheric Environment 10(10):891-896.

Nadarajah, S., and S. Kotz. 2004. The beta Gumbel distribution. Mathematical Problems in Engineering 2004(4):323-332.

Parnell, C. B. 1994. Testimony to Oklahoma Air Quality Council.

Peters, T., and R. Vanderpool. 1996. Modification and evaluation of the WINS impactor. Final Report. EPA Contract(68-D5):0040.

Pope III, C. A., R. T. Burnett, M. J. Thun, E. E. Calle, D. Krewski, K. Ito, and G. D. Thurston. 2002. Lung cancer, cardiopulmonary mortality, and long-term exposure to fine particulate air pollution. Journal of the American Medical Association 287(9):1132-1141.

Rader, D. J., and V. A. Marple. 1985. Effect of ultra-Stokesian drag and particle interception on impaction characteristics. Aerosol Science and Technology 4(2):141-156.

Ranade, M., M. Woods, F. Chen, L. Purdue, and K. Rehme. 1990. Wind tunnel evaluation of PM10 samplers. Aerosol Science and Technology 13(1):54-71.

Seaton, A., D. Godden, W. MacNee, and K. Donaldson. 1995. Particulate air pollution and acute health effects. The Lancet 345(8943):176-178.

APPENDIX A

EVALUATION OF FILTER MEDIA OPTIONS FOR HIGH VOLUME $PM_{2.5}$ SAMPLING

ABSTRACT

Cellulose, polytetrafluoride (PTFE) and glass fiber filter media were evaluated under controlled conditions to determine their suitability for high volume $PM_{2.5}$ sampling. Mounting tests were conducted in a laboratory environment. Mass losses were observed for all of three types of filters during the mounting process. The cellulose filter had the highest mass loss (6.25 mg), which would introduce significant bias in measured $PM_{2.5}$ concentrations, making this type filter unsuitable in high volume $PM_{2.5}$ sampling. The glass fiber filter had the lowest mass loss (0.21 mg), and glass fiber filters are now commercially available with alkalinity values similar to PTFE filters. Therefore, glass fibers filters similar in specification to Whatman EPM2000 filters should be considered acceptable substitutes for PTFE filters for use in high volume $PM_{2.5}$ sampling.

Key words: high volume $PM_{2.5}$, bias, filter, glass fiber, PTFE, cellulose

INTRODUCTION

Mass concentrations of ambient particulate matter are most often determined using filter-based sample collectors. The current federal reference method (FRM) for determining concentration of $PM_{2.5}$ utilizes 47mm polytetrafluoride (PTFE) filter (40 CFR 50 Appendix L). Interest has been expressed in developing a high volume (40 CFM) $PM_{2.5}$ sampler that would utilize 8 in. × 10 in. (0.2m × 0.2 m) filters, much like the high volume PM_{10} FRM sampler. The cost for 8 in. ×10 in. PTFE filters is non-trivial and may substantially increase the cost of $PM_{2.5}$ monitoring using a high volume sampler relative to cost if less expensive filter materials could be used.

Concerns regarding filter media selection for aerosol sampling are two-fold. First, during weighing, handling, and sampling, filters may lose mass, leading to a negative bias in the corresponding mass concentrations. The composition of a filter will affect its friability and, therefore, weight loss during these processes. Second, artifact formation may occur on some filter materials in which gas-to-particle conversions may lead to positive biases in mass concentration measurements. Oxidation of acidic gases (i.e., SO_2 and NO_2) and retention of nitric acid on the surface of alkaline glass fiber filters has been demonstrated by several studies (Appel et al. 1984; Pierson et al. 1980). However, glass fiber filters having similar alkalinity to PTFE filters approved for use in PM_{10} samplers are now commercially available, so artifact formation between these two filter materials should not vary substantially.

Rehme et al. (1984) investigated mass loss of three different filters: glass fiber filters, quartz filters and Teflon® filters, and found the use of quartz filters in high volume samplers was feasible. Teflon® filters had a tendency to clog during ambient sampling at concentration around 65 to 75 $\mu g/m^3$. These tests were conducted by Rehme et al. (1984) more than 30 years ago, and improvements in filter production processes may have occurred that could lead to less mass loss during handling and artifact formation more commensurate to that seen when using quartz or PTFE filters. The objective of this paper is to compare filter handling losses between recently-manufactured PTFE, glass fiber, and cellulose filters to determine their suitability for use in a high volume $PM_{2.5}$ sampler.

METHODS

Mass losses associated with handling of three different filter materials were assessed to determine the potential bias introduced by such losses. High volume filters (i.e., 8 in. x 10 in.) made of PTFE membrane (Whatman TE 36), cellulose (Whatman Grade 42), and glass fiber (Whatman EPM2000) were evaluated. Ten filters of each type were subjected to a mounting test to determine the magnitude of weight loss due to placement on a filter cartridge (Part No. TE-3000; Tisch Environmental Inc.; Cleves, Ohio) which protects the filter and provides structural support for the filter while in the sampler.

Each filter was conditioned in an environmental chamber (21±2 ^{o}C; 35±5% RH) for 48 hours prior to testing. After conditioning, each filter was placed into the filter cartridge and removed 10 times. No air was passed through the filter. Filters were weighed before and after each placement on the cartridge, rendering 11 weights per filter. Filters were weighed in the environmental chamber on a Mettler MX-5 microbalance (Mettler-Toledo Inc., Columbus, OH) after being passed through an anti-static device. The MX-5 microbalance was leveled on a marble table and housed inside a Plexiglass box to minimize the effects of air currents and vibrations. To reduce recording errors, weights were digitally transferred from the microbalance directly to a spreadsheet. Technicians wore latex gloves and a particulate respirator mask to avoid contamination. Quality control procedures required that filters be weighed three times each in batches of ten. If the standard deviation of the weights for a given filter exceeded 30 μg, the filter was weighed again.

Measured concentrations of $PM_{2.5}$ may be calculated as:

$$C = \frac{m_{PM} + m_{bias,art} - m_{bias,handling}}{Q \cdot t} \quad (20)$$

where: C = measured concentration of $PM_{2.5}$ ($\mu g/m^3$),

m_{PM} = mass of PM collected on the filter (µg),

$m_{bias,art}$ = mass of bias introduced by artifact formation on the filter (µg),

$m_{bias,handling}$ = mass of bias introduced by loss of mass during filter handling (µg), and

Q = flow rate of the sampler (m^3/min), and

t = sampling period (min).

For this study, bias due to artifact formation ($m_{bias,art}$) was neglected because the glass fiber filters tested had similar alkalinity (maximum: 25 µeg/g of filter(Whatman 2002)) to PTFE filters (maximum: < 25 µeg/g of filter (Whatman 2009)) such that the magnitude of artifact bias should be similar between the filter types. The potential bias introduced by filter handling ($m_{bias,handling}$) was evaluated at the threshold for National Ambient Air Quality Standards (NAAQS) for $PM_{2.5}$, where sampling bias has the potential to alter designation of a region between "attainment" and "non-attainment" for the $PM_{2.5}$ NAAQS. Therefore, bias was evaluated for a $PM_{2.5}$ concentration (C) of 12 $\mu g/m^3$ (USEPA 2012) and a volumetric flow rate (Q) of 40 CFM over a 24-hour sampling period (t). Detailed measurements are on APPENDIX C.

RESULTS AND DISCUSSION

Within each weighing event, the distributions of mass losses were analyzed for normality using the Shapiro-Wilk test. Two outliers were removed from the dataset for cellulose filters. All other data were normally distributed. The average mass lost during each of 10 handling procedures is shown in Figure 11, while the initial filter weight and average total mass lost during the ten mounting procedures is shown in Table 11.

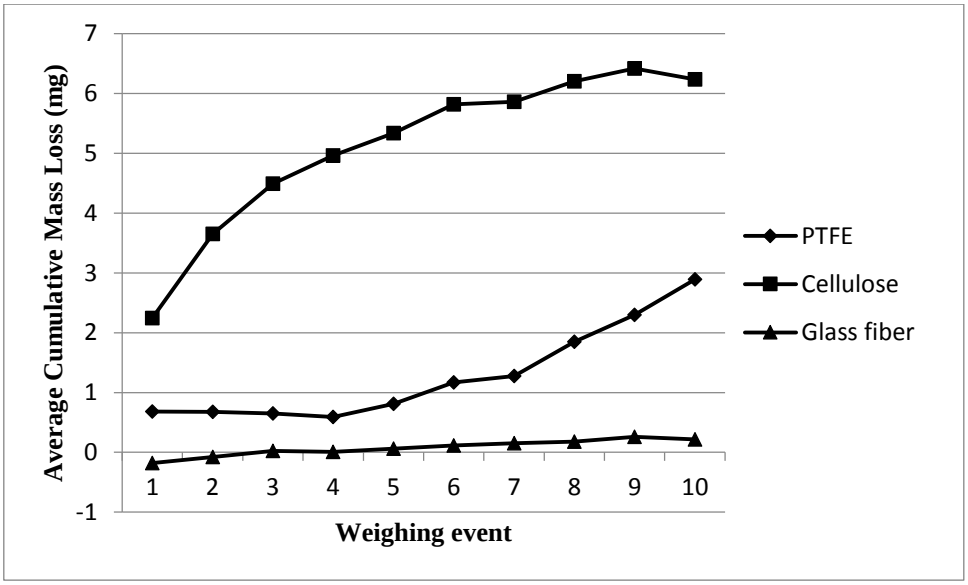

Figure 11. Cumulative mass loss over ten filter mounting and weighing events.

Table 11. Mass changes due to ten consecutive filter mounting and weighing events

Filter type	Pre-weight mass of filter (mg)	Average mass loss after 10 mounting procedures (mg)	Standard deviation of mass change (mg)	Corresponding bias in 24-hr mass concentration ($\mu g/m^3$)

Table 11. Continued

PTFE	17,829.84	2.89	2.96	-1.77
Cellulose	19,555.87	6.25	0.38	-3.81
Glass fiber	18,219.13	0.21	0.50	-0.13

Although cellulose filters may offer some price advantage compared with PTFE filter, the high mass loss due to filter mounting (6.25 mg over 10 mounting events) will result in a non-trivial bias in mass concentration (3.81 $\mu g/m^3$). Compared with the current $PM_{2.5}$ NAAQS annual standard of 12 $\mu g/m^3$, this bias would represent 32% measurement bias in NAAQS determination which renders cellulose filters unsuitable in high volume $PM_{2.5}$ sampling.

Contrary to the results reported by Rehme et al. (1984), less mass loss was measured during handling of glass fiber filters than PTFE filters. The average mass loss of glass fiber filters in this study was 0.21mg, while the filters (Schleicher & Schuell BioScience, Inc.; Keene, N.H.) analyzed by Rehme et al. (1984) lost 0.81mg during comparable tests. Given the composition of PTFE and glass fiber filters and the change in the trend of measured mass loss of PTFE filters after the fifth weighing event, it seems likely that observed differences in mass loss between PTFE and glass fiber filters may be the result of differences in static charge between the PTFE and glass fiber filters rather than real loss of mass. Although all filters were passed through an antistatic device before weighing, the size of the 8 in. x 10 in. filters makes it difficult for such systems to alleviate all static charge present.

Figure 12 shows the mass loss between each successive filter weighing event. For each kind of filter, the mass losses (or gain) of first event were highest among the ten weighing events. Instead of mass loss, the glass fiber gained mass (0.18mg) in the first weighing event. The possible reason is that the mass gain of moisture absorbed on the extended surface due to fragile nature of glass overweighs mass loss of glass fiber. The mass loss of cellulose filter (2.24mg) was significantly higher than mass loss of PTFE (0.68mg).

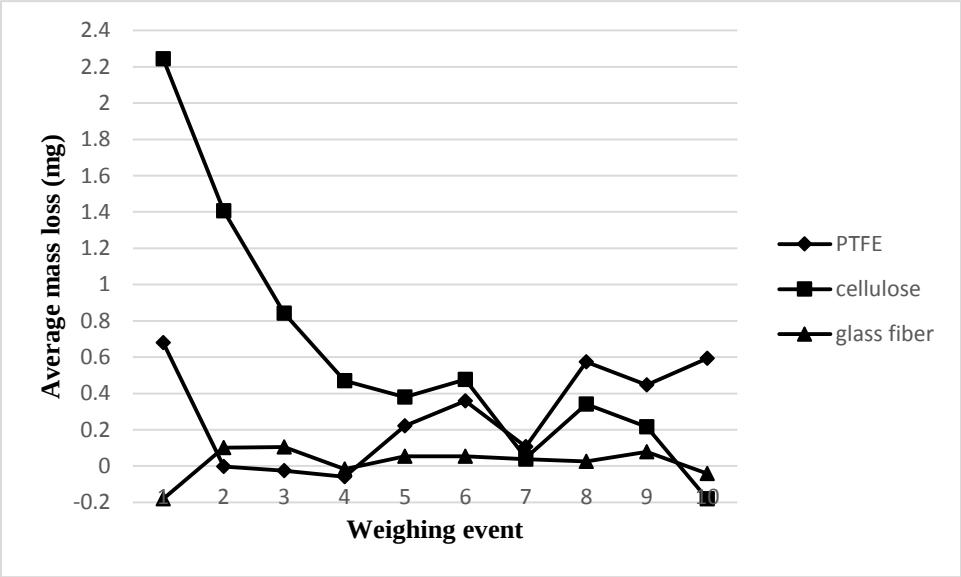

Figure 12. Mass loss between each successive filter weighing event.

CONCLUSION

Due to high mass loss during handling process, the cellulose filters tested in this study are unsuitable for high volume $PM_{2.5}$ sampling. Glass fiber filters demonstrated a lower mass loss than PTFE filters during handling, and glass fiber filters are now commercially available with alkalinity values similar to PTFE filters. Therefore, glass

fiber filters similar in specification to Whatman EPM2000 filters should be considered acceptable substitutes for PTFE filters for use in high volume $PM_{2.5}$ sampling.

DISCLAIMER

Mention of trade names or commercial products in this manuscript is solely for the purpose of providing specific information and does not imply recommendation or endorsement by the U.S. Department of Agriculture.

REFERENCES

Appel, B., Tokiwa, Y., Haik, M., Kothny, E. (1984). Artifact particulate sulfate and nitrate formation on filter media. *Atmospheric Environment* (1967) 18:409-416.

Pierson, W. R., W. W. Brachaczek, T. J. Korniski, T. J. Truex, and J. W. Butler. 1980. Artifact formation of sulfate, nitrate, and hydrogen ion on backup filters: Allegheny Mountain experiment. *Journal of the Air Pollution Control Association* 30(1):30-34.

Rehme, K., C. Smith, M. Beard, and T. Fitz-Simons. 1984. *Investigation of Filter Media for Use in the Determination of Mass Concentrations of Ambient Particulate Matter*. Environmental Monitoring Systems Laboratory, US Environmental Protection Agency.

Whatman (2002). TechnicalNotePM10Filters. http://www.whatman.com/References/TechnicalNotePM10Filters.pdf.

Whatman (2009). PM 2.5 Air Monitoring Membrane. http://www.whatman.com/PRODPM25AirMonitoringMembrane.aspx.

USEPA (2012). Code of Federal Regulations. National Ambient Air Quality Standards. 40 CFR Part 50. Washington D. C.: U.S. Government Printing Office. https://www.epa.gov/criteria-air-pollutants/naaqs-table.

APPENDIX B

CALCULATIONS OF DISTRIBUTION FUNCTIONS TO MODEL FEDERAL REFERENCE METHOD SAMPLER

Table 12. Distribution functions to fit FRM PM2.5 sampler performance(FRM to Folded normal)

AED(μm)	efficiencies						
	FRM	lognormal (best fit)	lognormal (d50=2.5, slope=1.3)	Weibull	Gamma	Dagum distribution	Folded normal
0.5	1	1.000	1.000	1.000	1.000	1.000	1.000
0.625	0.999	1.000	1.000	1.000	1.000	1.000	1.000
0.75	0.998	1.000	1.000	1.000	1.000	0.999	1.000
0.875	0.997	1.000	1.000	1.000	1.000	0.999	1.000
1	0.995	1.000	1.000	0.999	1.000	0.997	1.000
1.125	0.991	1.000	0.999	0.997	1.000	0.995	0.999
1.25	0.987	1.000	0.996	0.994	1.000	0.990	0.999
1.375	0.98	1.000	0.989	0.989	0.999	0.983	0.996
1.5	0.969	0.999	0.974	0.980	0.997	0.972	0.991
1.675	0.954	0.990	0.937	0.956	0.985	0.946	0.973
1.75	0.932	0.980	0.913	0.941	0.974	0.931	0.959
1.875	0.899	0.948	0.864	0.906	0.940	0.897	0.924
2	0.854	0.891	0.802	0.856	0.883	0.851	0.870
2.125	0.791	0.805	0.732	0.789	0.800	0.790	0.793
2.25	0.707	0.694	0.656	0.701	0.693	0.709	0.695
2.375	0.602	0.569	0.578	0.596	0.572	0.606	0.580
2.5	0.48	0.443	0.500	0.476	0.448	0.484	0.458
2.625	0.351	0.328	0.426	0.351	0.333	0.350	0.340
2.75	0.23	0.232	0.358	0.235	0.234	0.225	0.236
2.875	0.133	0.157	0.297	0.138	0.156	0.129	0.152
3	0.067	0.103	0.244	0.069	0.099	0.068	0.091
3.125	0.03	0.064	0.198	0.029	0.060	0.035	0.050
3.25	0.012	0.039	0.159	0.009	0.035	0.017	0.025
3.375	0.004	0.023	0.126	0.002	0.019	0.009	0.012
3.5	0.001	0.013	0.100	0.000	0.010	0.005	0.005
3.625	0	0.007	0.078	0.000	0.005	0.002	0.002
3.75	0	0.004	0.061	0.000	0.003	0.001	0.001
3.875	0	0.002	0.047	0.000	0.001	0.001	0.000
4	0	0.001	0.037	0.000	0.001	0.000	0.000
4.125	0	0.001	0.028	0.000	0.000	0.000	0.000
4.25	0	0.000	0.022	0.000	0.000	0.000	0.000

Table 12. Continued

AED(μm)	efficiencies						
	FRM	lognormal (best fit)	lognormal (d50=2.5, slope=1.3)	Weibull	Gamma	Dagum distribution	Folded normal
4.375	0	0.000	0.016	0.000	0.000	0.000	0.000
4.5	0	0.000	0.013	0.000	0.000	0.000	0.000
4.625	0	0.000	0.010	0.000	0.000	0.000	0.000
4.75	0	0.000	0.007	0.000	0.000	0.000	0.000
4.875	0	0.000	0.005	0.000	0.000	0.000	0.000
5	0	0.000	0.004	0.000	0.000	0.000	0.000
5.125	0	0.000	0.003	0.000	0.000	0.000	0.000
5.25	0	0.000	0.002	0.000	0.000	0.000	0.000
5.375	0	0.000	0.002	0.000	0.000	0.000	0.000
5.5	0	0.000	0.001	0.000	0.000	0.000	0.000
5.625	0	0.000	0.001	0.000	0.000	0.000	0.000
5.75	0	0.000	0.001	0.000	0.000	0.000	0.000

Table 13. Distribution functions to fit FRM PM2.5 sampler performance (Rayleigh to Logistic)

AED(μm)	efficiencies					
	Rayleigh	Log-logistic	Gumbel	Shifted Gompertz	Fréchet	Logistic
0.5	0.966	1.000	1.000	1.000	1.000	1.000
0.625	0.948	1.000	1.000	1.000	1.000	1.000
0.75	0.926	1.000	1.000	1.000	1.000	0.999
0.875	0.900	1.000	1.000	1.000	1.000	0.999
1	0.871	1.000	1.000	1.000	1.000	0.998
1.125	0.840	1.000	1.000	1.000	1.000	0.996
1.25	0.807	0.999	1.000	1.000	1.000	0.994
1.375	0.771	0.998	1.000	1.000	1.000	0.989
1.5	0.734	0.994	1.000	1.000	1.000	0.982
1.675	0.680	0.981	0.998	0.998	1.000	0.964
1.75	0.656	0.971	0.994	0.994	1.000	0.951
1.875	0.616	0.942	0.971	0.971	0.992	0.920
2	0.577	0.891	0.913	0.913	0.948	0.872
2.125	0.537	0.813	0.814	0.814	0.844	0.802
2.25	0.498	0.705	0.687	0.687	0.697	0.705
2.375	0.460	0.575	0.552	0.552	0.544	0.587
2.5	0.423	0.442	0.426	0.426	0.411	0.457
2.625	0.387	0.322	0.318	0.318	0.304	0.333
2.75	0.353	0.226	0.232	0.232	0.224	0.228
2.875	0.321	0.155	0.167	0.167	0.164	0.149
3	0.290	0.105	0.119	0.119	0.121	0.094
3.125	0.261	0.071	0.083	0.083	0.090	0.058
3.25	0.234	0.048	0.058	0.058	0.067	0.035
3.375	0.209	0.033	0.041	0.041	0.051	0.021
3.5	0.185	0.023	0.028	0.028	0.039	0.013
3.625	0.164	0.016	0.020	0.020	0.030	0.008
3.75	0.144	0.011	0.014	0.014	0.023	0.004
3.875	0.127	0.008	0.009	0.009	0.018	0.003
4	0.111	0.006	0.007	0.007	0.014	0.002
4.125	0.096	0.004	0.004	0.004	0.011	0.001
4.25	0.083	0.003	0.003	0.003	0.009	0.001
4.375	0.072	0.002	0.002	0.002	0.007	0.000
4.5	0.062	0.002	0.001	0.001	0.006	0.000

Table 13. Continued

AED(μm)	efficiencies					
	Rayleigh	Log-logistic	Gumbel	Shifted Gompertz	Fréchet	Logistic
4.625	0.053	0.001	0.001	0.001	0.005	0.000
4.75	0.045	0.001	0.001	0.001	0.004	0.000
4.875	0.038	0.001	0.000	0.000	0.003	0.000
5	0.032	0.001	0.000	0.000	0.002	0.000
5.125	0.027	0.000	0.000	0.000	0.002	0.000
5.25	0.023	0.000	0.000	0.000	0.002	0.000
5.375	0.019	0.000	0.000	0.000	0.001	0.000
5.5	0.016	0.000	0.000	0.000	0.001	0.000
5.625	0.013	0.000	0.000	0.000	0.001	0.000
5.75	0.011	0.000	0.000	0.000	0.001	0.000

Table 14. Distribution functions to fit FRM PM10 sampler performance (FRM to Folded normal)

AED(μm)	efficiencies						
	FRM	lognormal (best fit)	lognormal (d50=10, slope=1.5)	Weibull	Dagum	Logistic	Folded normal
1	1	1.000	1.000	0.999	0.992	0.973	0.988
1.5	0.949	1.000	1.000	0.996	0.984	0.968	0.981
2	0.942	1.000	1.000	0.992	0.973	0.961	0.973
2.5	0.933	0.999	1.000	0.985	0.960	0.953	0.964
3	0.922	0.998	0.999	0.975	0.945	0.943	0.953
3.5	0.909	0.993	0.995	0.963	0.928	0.932	0.940
4	0.893	0.984	0.988	0.947	0.909	0.918	0.924
4.5	0.876	0.969	0.976	0.927	0.887	0.902	0.906
5	0.857	0.946	0.956	0.904	0.864	0.883	0.885
5.5	0.835	0.917	0.930	0.877	0.840	0.862	0.860
6	0.812	0.880	0.896	0.846	0.813	0.837	0.833
6.5	0.786	0.837	0.856	0.813	0.785	0.808	0.802
7	0.759	0.790	0.810	0.775	0.754	0.776	0.768
7.5	0.729	0.739	0.761	0.735	0.723	0.740	0.731
8	0.697	0.687	0.709	0.693	0.689	0.701	0.691
8.5	0.664	0.634	0.656	0.649	0.654	0.658	0.649
9	0.628	0.581	0.603	0.603	0.617	0.613	0.605
9.5	0.59	0.530	0.550	0.556	0.579	0.565	0.560
10	0.551	0.481	0.500	0.509	0.539	0.517	0.514
10.5	0.509	0.435	0.452	0.462	0.498	0.468	0.468
11	0.465	0.392	0.407	0.416	0.455	0.419	0.422

Table 14. Continued

AED(μm)	efficiencies						
	FRM	lognormal (best fit)	lognormal (d50=10, slope=1.5)	Weibull	Dagum	Logistic	Folded normal
12	0.371	0.315	0.326	0.328	0.364	0.328	0.334
13	0.269	0.250	0.259	0.250	0.268	0.248	0.254
14	0.159	0.197	0.203	0.183	0.166	0.182	0.186
15	0.041	0.155	0.159	0.128	0.066	0.131	0.130
16	0	0.121	0.123	0.086	0.010	0.092	0.087
17	0	0.094	0.095	0.055	0.001	0.064	0.056
18	0	0.073	0.074	0.034	0.000	0.044	0.034
20	0	0.044	0.044	0.011	0.000	0.021	0.011
22	0	0.027	0.026	0.003	0.000	0.010	0.003
24	0	0.016	0.015	0.001	0.000	0.004	0.001
26	0	0.010	0.009	0.000	0.000	0.002	0.000
28	0	0.006	0.006	0.000	0.000	0.001	0.000
30	0	0.004	0.003	0.000	0.000	0.000	0.000
35	0	0.001	0.001	0.000	0.000	0.000	0.000
40	0	0.000	0.000	0.000	0.000	0.000	0.000
45	0	0.000	0.000	0.000	0.000	0.000	0.000

Table 15.Distribution functions to fit FRM PM10 sampler performance (Log-logistic to Gamma)

AED(μm)	efficiencies				
	Log-logistic	Gumbel	Shifted Gompertz	Fréchet	Gamma
1	1.000	0.999	0.999	1.000	1.000
1.5	0.999	0.998	0.999	1.000	1.000
2	0.998	0.995	0.996	1.000	0.998
2.5	0.996	0.991	0.992	1.000	0.996
3	0.992	0.983	0.986	1.000	0.990
3.5	0.984	0.973	0.975	1.000	0.981
4	0.974	0.958	0.961	1.000	0.967
4.5	0.958	0.938	0.941	0.998	0.948
5	0.938	0.913	0.916	0.989	0.923
5.5	0.911	0.883	0.886	0.967	0.894
6	0.879	0.848	0.851	0.930	0.859
6.5	0.840	0.808	0.811	0.879	0.820
7	0.797	0.766	0.768	0.819	0.777
7.5	0.748	0.720	0.722	0.753	0.731
8	0.696	0.673	0.674	0.687	0.684
8.5	0.643	0.626	0.626	0.622	0.635
9	0.588	0.578	0.578	0.562	0.586
9.5	0.535	0.531	0.531	0.506	0.538
10	0.484	0.486	0.485	0.456	0.491
10.5	0.435	0.442	0.442	0.411	0.445
11	0.390	0.401	0.400	0.370	0.402

Table 15. Continued

AED(μm)	efficiencies				
	Log-logistic	Gumbel	Shifted Gompertz	Fréchet	Gamma
12	0.311	0.327	0.326	0.302	0.322
13	0.247	0.263	0.262	0.248	0.254
14	0.196	0.210	0.208	0.206	0.197
15	0.156	0.166	0.165	0.172	0.150
16	0.125	0.131	0.130	0.145	0.113
17	0.101	0.102	0.101	0.123	0.084
18	0.082	0.080	0.079	0.105	0.062
20	0.055	0.048	0.048	0.079	0.032
22	0.038	0.029	0.029	0.060	0.016
24	0.027	0.017	0.017	0.047	0.008
26	0.020	0.010	0.010	0.038	0.004
28	0.015	0.006	0.006	0.031	0.002
30	0.011	0.004	0.004	0.025	0.001
35	0.006	0.001	0.001	0.016	0.000
40	0.004	0.000	0.000	0.011	0.000
45	0.002	0.000	0.000	0.008	0.000

APPENDIX C

THREE TYPES OF FILTERS MEASUREMENTS

Table 16. Measurements of PTFE filter

Filter ID	Pre-weight	Weight event				
		Weight 1	Weight 2	Weight 3	Weight 4	Weight 5
1	17774.39	17773.47	17774.12	17774.99	17775.47	17774.48
2	17744.92	17744.55	17744.86	17745.12	17745.12	17745.38
3	17785.49	17785.71	17786.14	17786.20	17786.34	17787.10
4	17812.31	17811.86	17811.64	17811.82	17810.96	17811.00
5	17863.00	17861.65	17861.33	17861.04	17861.04	17861.22
6	17784.96	17784.80	17784.95	17784.72	17785.01	17784.69
7	17841.10	17840.15	17840.42	17840.36	17840.70	17840.46
8	17825.02	17824.42	17824.31	17824.09	17824.64	17823.77
9	17968.79	17967.79	17967.57	17967.25	17967.59	17966.71
10	17898.46	17897.24	17896.33	17896.34	17895.66	17895.51
	(continued)	Weight 6	Weight 7	Weight 8	Weight 9	Weight 10
1		17775.62	17776.14	17775.52	17775.51	17775.44
2		17745.40	17745.56	17745.27	17745.37	17745.93
3		17785.72	17786.25	17785.10	17784.91	17784.67
4		17810.33	17809.71	17808.95	17807.19	17805.66
5		17861.01	17861.36	17861.05	17860.67	17860.30
6		17784.56	17784.23	17784.15	17783.72	17783.82
7		17839.92	17840.12	17839.86	17840.13	17838.71
8		17823.00	17822.67	17821.76	17821.47	17820.37
9		17966.14	17965.26	17964.52	17963.36	17962.52
10		17895.03	17894.36	17893.75	17893.14	17892.12

Table 17. Measurements of cellulose filter

Filter ID	Pre-weight	Weight event				
		Weight 1	Weight 2	Weight 3	Weight 4	Weight 5
1	19606.19	19607.69	19607.50	19606.95	19606.08	19605.50
2	19553.25	19550.55	19548.49	19548.12	19546.91	19546.47
3	19582.57	19578.70	19577.76	19577.22	19576.69	19576.73
4	19581.14	19577.26	19576.10	19575.96	19576.05	19575.49
5	19541.40	19539.64	19538.16	19537.07	19536.80	19536.41
6	19493.23	19490.55	19489.11	19487.91	19487.67	19487.67
7	19523.62	19520.98	19519.63	19518.63	19518.29	19517.53
8	19591.06	19591.18	19589.16	19586.21	19585.11	19585.08
9	19567.11	19563.81	19562.21	19562.01	19562.32	19561.63
10	19519.17	19515.94	19514.12	19513.75	19513.21	19512.83
	(continued)	Weight 6	Weight 7	Weight 8	Weight 9	Weight 10
1		19604.44	19603.84	19603.14	19602.27	19602.80
2		19546.65	19547.08	19546.90	19546.21	19546.68
3		19576.43	19575.82	19575.17	19575.78	19576.22
4		19575.23	19575.40	19575.13	19575.38	19575.61
5		19536.01	19536.03	19535.75	19535.62	19535.36
6		19487.27	19487.69	19487.26	19487.08	19486.93
7		19516.97	19517.58	19517.94	19517.95	19517.60
8		19585.09	19584.68	19584.49	19584.11	19584.50
9		19560.77	19560.97	19560.41	19560.08	19560.45
10		19511.71	19511.03	19510.52	19510.07	19510.20

Table 18. Measurements of glass fiber filter

Filter ID	Pre-weight	Weight event				
		Weight 1	Weight 2	Weight 3	Weight 4	Weight 5
1	18219.12	18219.52	18218.91	18218.80	18218.47	18218.55
2	18225.66	18225.14	18225.17	18225.05	18225.24	18224.96
3	18195.10	18195.13	18195.31	18194.94	18195.05	18195.23
4	18212.22	18212.55	18212.01	18212.09	18211.82	18212.06
5	18210.85	18211.21	18210.93	18210.82	18211.00	18210.82
6	18236.15	18236.38	18236.30	18236.19	18236.25	18236.22
7	18202.47	18202.93	18203.23	18202.95	18203.06	18202.94
8	18209.51	18209.65	18209.84	18209.57	18209.76	18209.66
9	18238.48	18238.37	18238.55	18238.46	18238.50	18238.18
10	18241.73	18242.21	18241.82	18242.16	18242.04	18242.04
	(continued)	Weight 6	Weight 7	Weight 8	Weight 9	Weight 10
1		18218.65	18218.02	18218.31	18218.15	18218.18
2		18225.10	18225.30	18224.70	18224.77	18224.97
3		18194.99	18194.77	18194.94	18195.00	18194.71
4		18211.93	18211.82	18211.92	18211.66	18211.94
5		18210.53	18210.44	18210.57	18210.37	18210.16
6		18236.25	18236.13	18236.01	18235.90	18235.78
7		18202.81	18203.05	18202.85	18203.15	18203.08
8		18209.68	18209.85	18209.66	18209.44	18209.73
9		18238.27	18238.42	18238.62	18238.47	18238.75
10		18241.92	18241.96	18241.92	18241.81	18241.84